NTNU – Trondheim
Norwegian University of
Science and Technology

Vortex Induced Vibrations of Slender Marine Structures

Maren Brunborg

Marine Technology
Submission date: June 2013
Supervisor: Carl Martin Larsen, IMT

Norwegian University of Science and Technology
Department of Marine Technology

NTNU Trondheim
Norwegian University of Science and Technology
Faculty of Engineering Science and Technology
Department of MarineTechnology

M.Sc. thesis 2013

for

Stud. tech. Maren Brunborg

VORTEX INDUCED VIBRATIONS OF SLENDER MARINE STRUCTURES

(Virvelindusert respons i slanke marine konstruksjoner)

VIV has been studied experimentally at MARINTEK/NTNU for almost two decades. These experiments include flexibly supported rigid cylinders, forced motion of rigid cylinders and long, flexible beams. The overall aim has been to improve the understanding of VIV and thereby establish a reliable response model for prediction of VIV. One result of this effort is the computer program VIVANA that can calculate fatigue damage caused by VIV for a large variety of slender marine structures.

Recent development of VIVANA has focused on 3D modelling, combined in-line and cross-flow response and how competing frequencies interact. Two options have been introduced to describe the competition between response frequency candidates; space sharing (concurrent response frequencies) and time sharing (consecutive response frequencies). Concurrent means that the competing frequencies are excited in specific zones along the structure where they are allowed to control the vortex shedding process, while consecutive allows each frequency to control the process along the entire length for a specific fraction of time. In reality we may observe a combination of the two classes of response, but a good model to describe the space/time/frequency process has so far not been established.

The two methods have been implemented in VIVANA, but the experience with the methods is still not extensive. It is therefore of interest to analyse data from previous experiments in order to gain information on how response frequencies occur in time and space. Also other parameters that can help to improve VIVANA are of interest to study through previous experiments.

The work might be divided into tasks as follows:

1. Literature study related to methods for analysis of measurements that can give information about response frequencies in time and space, and how the computer program VIVANA selects active frequencies and their interaction.

2. Analysis of measurements from the “NDP high mode” experiments should be carried out in order to describe frequency participation in time and space for selected cases. Also extract other information from these measurements that may be of importance for the understanding of VIV.

3. From the literature study, find aspects of the VIVANA analysis model that can be improved, and - if possible - use the information from NDP analyses to give recommendations for these areas of improvement.

The work may show to be more extensive than anticipated. Some topics may therefore be left out after discussion with the supervisor without any negative influence on the grading.

The candidate should in her/his report give a personal contribution to the solution of the problem formulated in this text. All assumptions and conclusions must be supported by mathematical models and/or references to physical effects in a logical manner.
The candidate should apply all available sources to find relevant literature and information on the actual problem.

The report should be well organised and give a clear presentation of the work and all conclusions. It is important that the text is well written and that tables and figures are used to support the verbal presentation. The report should be complete, but still as short as possible.

The final report must contain this text, an acknowledgement, summary, main body, conclusions and suggestions for further work, symbol list, references and appendices. All figures, tables and equations must be identified by numbers. References should be given by author name and year in the text, and presented alphabetically by name in the reference list. The report must be submitted in two copies unless otherwise has been agreed with the supervisor.

The supervisor may require that the candidate should give a written plan that describes the progress of the work after having received this text. The plan may contain a table of content for the report and also assumed use of computer resources.

From the report it should be possible to identify the work carried out by the candidate and what has been found in the available literature. It is important to give references to the original source for theories and experimental results.

The report must be signed by the candidate, include this text, appear as a paperback, and - if needed - have a separate enclosure (binder, DVD/ CD) with additional material.

Supervisor at NTNU is Professor Carl M. Larsen, while Jie Wu at MARINTEK may help with the data analyses.

Trondheim, February 2013

Carl M. Larsen

Submitted: January 2013
Deadline: 10 June 2013

Abstract

The main objective of this thesis is to study the behaviour of slender marine structures exposed to vortex induced vibrations (VIV). Especially the interaction between active response frequencies is important. This is done by analysing results from an experiment simulating VIV on a riser. Improved understanding of this phenomenon is important for the marine- and offshore industry as operations subsea and in deeper waters are in growth. Hence, a goal is to use findings from experiments in an attempt to improve VIVANA, a program predicting responses regarding VIV.

The first part of the thesis include an overview of ways to analyse and process measurements from experiments in order to gain information on VIV. A literature study on how VIVANA select active response frequencies and how they are predicted to interact, is also included.

Based on the first part, an analysis of results from the "High Mode VIV Test" carried out for the Norwegian Deepwater Programme (NDP), is performed. The main analysis contains generation of figures showing how the active response frequencies of the riser behaves in time and space. Two different current profiles with a number of velocities are used to obtain a large sample, which is necessary in the attempt to see a pattern. Also amplitude plots are made from the measurements, mainly to get information of dominating modes.

It was difficult to discover clear patterns for the frequency interaction in space and time. However, it can be seen signs of time- and space sharing, which more or less confirms the conclusions from former experiments, that the real response is a combination of these two approaches.

What turned out to be the most important finding in this thesis comes from calculating the added mass of the modelled riser. The dominating mode and dominating frequency for each case found from the mentioned plots, are used in this calculation to see how the added mass change for increasing current velocity and mode. The results show that added mass seems to stabilize around a constant value for higher current velocities and modes. If this can be verified, it is valuable information because it means that a crucial part of the analysis in VIVANA can be simplified and hence improve the program.

Sammendrag

Hensikten med denne oppgaven er å studere oppførselen til slanke marine konstruksjoner når de er utsatt for virvelinduserte svingninger (VIV). Det er særlig viktig å se på samspillet mellom aktive responsfrekvenser. I denne oppgaven er dette undersøkt ved å analysere resultater fra et eksperiment som simulerer VIV på en riser-modell. Forbedret kunnskap om dette fenomenet er særlig viktig for den marine industrien med tanke på at operasjoner offshore stadig gjøres i større grad under vann og på større vanndyp. Derfor er det et mål at observasjoner gjort fra eksperimentets målinger skal kunne brukes til å forbedre VIVANA, som er et mye brukt program for å forutsi respons fra VIV på slanke kontruksjoner.

Den første delen av denne oppgaven omfatter en oversikt over måter man kan analysere og prosessere målinger fra eksperimenter på for å oppnå informasjon om VIV. Det er også gjort et litteraturstudie av hvordan VIVANA gjennom sin analyse velger ut aktive responsfrekvenser og hvordan disse er satt til å virke i forhold til hverandre.

Basert på den første delen er det videre utført en analyse av resultater fra "High Mode VIV Test" gjort for "Norwegian Deepwater Programme" (NDP). Hovedaspektet ved denne analysen er generering av figurer som viser hvordan de aktive responsfrekvensene for denne riseren oppfører seg i tid og sted. To ulike strømprofiler med flere hastigheter er brukt slik at oppførselen kan studeres i mange tilfeller, for muligens å kunne avdekke et mønster. Plot som viser amplitudene til riserens bevegelse er også laget fra målingene. Fra disse kan man blant annet få informasjon om hvilke moder som er dominerende i løpet av en tidsserie.

Tolkningen av de genererte figurene for aktive frekvenser viser at det er vanskelig å se/gjenkjenne tydelige mønstre som kan si noe om samspillet mellom dem, som for eksempel tilnærmingsmetodene VIVANA bruker på dette området. Og derfor kan det i denne delen av oppgaven ikke konkluderes med noe særlig annet enn at den faktiske oppførselen for en riser i VIV-tilstand er kompleks og vanskelig å modellere korrekt, noe som er konklusjonen i flere liknende arbeid utført tidligere. Men for noen av de undersøkte tilfellene kan det allikevel sees spor av noe som ligner på måten VIVANA modellerer frekvensene på, slik at det kan ha noe for seg i et videre arbeid å sammenligne resultater fra denne oppgaven med en analyse i VIVANA.

Det som imidlertid viser seg å være den viktigste og mest interessante observasjonen fra denne oppgaven kommer fra utregningen av "added mass" for risermodellen. Verdiene, som er plottet i en figur som viser endringen i added mass

for økende strømhastighet og mode, viser at added mass ser ut til å stabilisere seg rundt en konstant verdi for tilfeller med høye hastigheter og moder. Hvis dette kan verifiseres, er det en verdifull observasjon da det betyr at en viktig del av analysen i VIVANA kan forenkles, og dermed forbedre programmet.

Acknowledgement

This thesis is written during the spring-semester of 2013 as the finishing part of the Masters Degree in Marine technology at Department of Marine Technology, Norwegian University of Science and Technology.

During the work I have had a good follow-up from my supervisor Prof. Carl Martin Larsen, which I would like to thank. He is a great motivator due to his wide knowledge, experience and enthusiasm within the scope of this thesis. We also had a good collaboration through the process by adjusting the scope along the way and finding further usage of obtained results.

In addition I want to thank Jie Wu at MARINTEK for providing most of the codes in MATLAB that has been the basis for the analyses performed in this thesis. He has also been helpful and always available for questions regarding the codes.

Maren Brunborg

Contents

Nomenclature

Latin symbols

$\frac{A}{D}$	Amplitude ratio (non-dimensional amplitude)
C_e	Excitation force coefficient
$C_{e,CF}$	Excitation force coefficient, cross-flow
C_L	Lift coefficient
D	Diameter of structure (riser)
EI	Bending stiffness
f_{0i}	Eigenfrequency no. i
$\hat{f}_i$	Non-dimensional frequency
f_{osc}	Oscillation frequency
f_{st}	Strouhal frequency, vortex shedding frequency
Hz	Hertz, frequency unit: $[\frac{1}{s}]$
k	Iteration step in VIVANA to find response frequencies
k_B	Stiffness of beam without tension
k_{BS}	Stiffness of beam with tension
k_S	Stiffness of string with tension
L, l	Length of structure (riser)
L/D	Length-to-diameter ratio
L_E	Length of an excitation zone along the riser
m	Mass
m_A	Added mass
$q_i(t)$	Time independent weight factor, mode i
$\boldsymbol{q}$	Vector containing N weight factors, one for each of the N mode shapes
St	Strouhal number
T	Tension

U, U_c Current velocity

U_{max} Max velocity of sheared current

$w(x,t)$ Displacement at position x at time t

$\boldsymbol{w}$ Vector containing M displacement-values, one for each of the M positions along the structure

Greek symbols

$\boldsymbol{\varphi}$ MxN-matrix containing N mode shapes, for M positions along the structure

$\varphi_i(x)$ Mode shape at position x, mode i

ω_B Eigenfrequency of beam without tension

ω_{BS} Eigenfrequency of beam with tension

ω_S Eigenfrequency of string with tension

Abbreviations

CF Cross-flow

IL In-line

NDP Norwegian Deepwater Programme

NTNU Norwegian University of Science and Technology

RMS Root Mean Square

VIV Vortex Induced Vibrations

Chapter 1

Introduction

1.1 Motivation

The phenomenon of vortex induced vibrations and the response it may give a slender marine structure is still not fully understood. Especially, there are uncertainty of how different active response frequencies interact and it is not found a clear pattern that can describe this correctly, only some approaches.

As risers and other types of slender structures are commonly used in various subsea developments and operations, which is an industry in growth, it is important to gain more detailed knowledge of their response to VIV. Hence, new knowledge is important for improving existing tools for prediction of VIV. By investigating results from a VIV - model test, one may be able to find patterns and conclusions that can be implemented in, and hence improve, such tools.

VIVANA is a commonly used computer program that predicts responses related to VIV. Related to the mentioned problems by prediction of VIV, it is especially how the active and dominating response frequencies are chosen and how they are modelled to interact that is the core of the desired improvement in VIVANA. A study of how VIVANA execute these parts of the analysis today is an important part of this thesis in order to understand how the program may be improved and what could be explored from the model test results.

1.2 Background

This thesis is partly a continued work from the project thesis, Brunborg [2012]. The project thesis was mainly a literature study of general aspects of VIV, how it can be predicted and which experiments that is commonly performed. Since such a comprehensive pre-study of the theory is already done, it is not included much of background theory in this thesis. The project thesis is meant to be a complementary document to this thesis. However, a short summary of the basic theory is included in the following.

As understood from the name, vortex induced vibrations are responses on a structure due to vortices. The vortices are formed on the surface of, and shed behind, a slender structure (often with circular cross-section) that is exposed to a flow. The shape and size of both the structure and the current are some of the factors influencing the vortex shedding. The forces induced on the structure from the vortices may appear in cross-flow (CF) and/or in-line(IL) directions, creating an oscillating movement that may cause fatigue and drag amplification. It is known that this oscillating movement may appear at several frequencies. The big question is how they interact, as one position at the structure can only experience one frequency at a time. Two approaches for organizing this interaction, that for instance is used by VIVANA, is called space- and time sharing. Space sharing, or concurrent frequencies, implies that several response frequencies act at the same time, but each is only excited at a specific zone along the structure. Time sharing, or consecutive frequencies, implies that one frequency controls the motion along the entire length of the structure, but only for a limited time period. After a while, a different frequency will take over and control the process. More detailed and extensive theory is found in Brunborg [2012].

In addition to the literature study, the project thesis also comprises one analysis of data from a VIV model test of a riser. The case analysed seemed to have too low current velocity in order to see significant patterns in frequency competition. With that in mind, cases with higher current velocities, and hence higher modes dominating, should be investigated further. It is also necessary to look at both uniform and sheared current profile, trying to find differences/patterns also in this matter. In addition to concluding that several cases must be investigated, an important aspect from the project thesis was gaining the necessary knowledge to actually execute analyses of measurements.

Chapter 2

Ways of analysing measurements to study VIV

There are many ways to analyse data from experiments, all depending on what you are to investigate and what you want to show. In this work, the goal is to find out more about how VIV actually makes the riser behave. Consequently, in this chapter it is discussed a few ways to process measurements to gain information of the behaviour regarding VIV.

2.1 Time development for active frequencies

A good and illustrative way of looking at the VIV behaviour of a specific test, is to make a plot showing the time development of the oscillation frequencies along the structure. From such a plot one can observe which frequencies that dominate and how the complete frequency picture changes with time. This type of analysis is a suggestion made in Larsen et al. [2012]., and an example of this kind of plot is shown below.

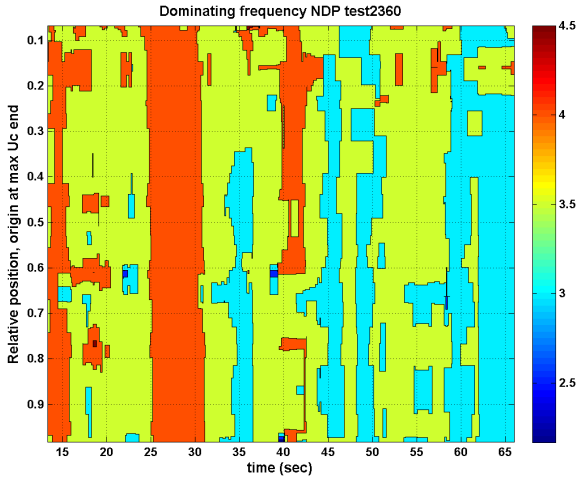

Figure 2.1: Example of contour plot showing development of oscillation frequencies in time and along a structure.

This kind of figure is a very good tool for discovering space- and time sharing, two approaches for organizing several dominating frequencies as briefly described in section 1.1 in the introduction. By generating several plots like this, for different velocities and shapes of current, a powerful and clear picture of the behaviour of a structure in VIV condition is gained. Important aspects to investigate is whether one can see a pattern for cases with a specific current profile, and also compare the findings for different profiles to look for differences/similarities. It is also important to look for patterns in terms of increasing velocities.

2.2 Time development for amplitudes

Another powerful way of studying the behaviour of a structure in VIV condition, is to make a plot of displacement amplitudes. This may be plotted as a contour map against both time and position along a riser, as for the active frequencies. From such plots one is able to see if the oscillation of the structure has a standing or travelling wave pattern. And from that one may find positions along the structure which are interesting. For example, it may be desirable to try to find a statistical description of the amplitudes at positions where the wave pattern is not easily defined. Hence, a small part of the VIV condition may be described better than before. [Larsen [2013]]

It is also possible to see approximately which mode order is present, and if/how this changes with time. Knowing the actual mode order for several cases is useful

as it may be used further in various investigations, such as calculating the actual added mass.

Figure 2.2 shows an example of such a plot, taken from Wu [2011].

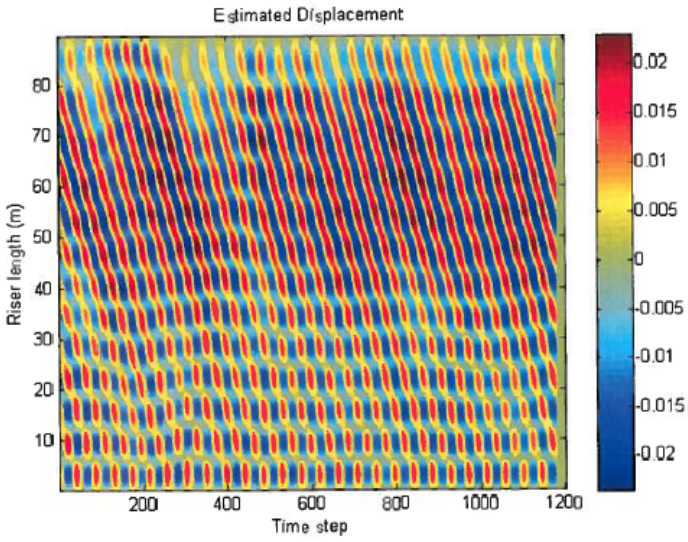

Figure 2.2: Example of plot showing displacement amplitude in time and along a structure. From Wu [2011].

Amplitude plots can also be made from values other than displacement, for instance strain which is often the raw measurements in experiments.

2.3 Modal analysis

Another way of improving the understanding of VIV is to gain information about the mode competition. As explained in the previous section, a rough estimation of which mode is dominating in a time series can be seen from an amplitude plot. But in order to see and study the time varying shape of a structure in detail, a modal decomposition needs to be made, to see which modes dominate. How to do this with results from a model test, as opposed to a theoretical modal analysis, is explained briefly in the following. The explanation is based on theory from Lie & Kaasen [2006], Kristiansen & Lie [2005] and chapter 7 in Larsen [2009].

The basis for this method is the equation representing modal superposition:

$$w(x,t) = \sum_{i=1}^{N} \varphi_i(x) q_i(t) \tag{2.1}$$

Here w(x,t) is the displacement at position x along the structure at time t. $\varphi_i(x)$ is known eigenmodes (mode shapes) and $q_i(t)$ is time dependent weight factors. These weight factors decide how strongly each eigenmode is represented in the final deformation shape at any time, and the goal is to find these. From model tests one have time series of displacements or other measurements that can be transformed into displacements. Consequently the deformation of the model is known at the points where the measurement instruments are placed, which means that the corresponding weight factors can be found in the time interval used in the test.

Going further in the explanation of finding the weights, equation 2.1 is written in matrix/vector form:

$$\boldsymbol{\varphi}\mathbf{q} = \mathbf{w} \tag{2.2}$$

where

$$\boldsymbol{\varphi} = \begin{pmatrix} \varphi_{1,1} & \varphi_{1,2} & \cdots & \varphi_{1,N} \\ \varphi_{2,1} & \varphi_{2,2} & \cdots & \varphi_{2,N} \\ \vdots & \vdots & \ddots & \vdots \\ \varphi_{M,1} & \varphi_{M,2} & \cdots & \varphi_{M,N} \end{pmatrix}, \mathbf{q} = \begin{bmatrix} q_1(t) \\ q_2(t) \\ \vdots \\ q_N(t) \end{bmatrix}, \mathbf{w} = \begin{bmatrix} w_1(t) \\ w_2(t) \\ \vdots \\ w_M(t) \end{bmatrix} \tag{2.3}$$

Here $\boldsymbol{\varphi}$ is a MxN-matrix, presenting N mode shapes and their position at each of the M positions along the structure with known values of displacements. $\boldsymbol{q}$ is the column vector containing N weight factors, representing participation in the final deformation at time instant t for each mode shape. $\boldsymbol{w}$ is the column vector containing M displacements, one for each position along the structure at time t. This is the product of the matrix/vector equation.

As mentioned it is the weight factor that is the goal to find, which can provide useful information of the mode competition in time. This implies that equation 2.2 must be transformed to

$$\mathbf{q} = \boldsymbol{\varphi}^{-1}\mathbf{w} \tag{2.4}$$

This equation then needs to be solved for all time values, to find the time development of the weight factors. To be able to solve the equation the N number of mode shapes can not be higher than the M number of instruments along the model. If N=M, the $\boldsymbol{\varphi}$-matrix is square and it is straight forward matrix solving to obtain the weight factors, like equation 2.4. If N<M, there are more equations than unknown variables and the weight factors can be found by using "Least Squares Method".

It would be natural to think that any mode could be used as long as the total number of modes was less than or equal to the number of measurement-positions. For instance that for a case with 20 instruments along a structure, not necessarily just mode 1-20 could be used, but also 10-30 if it was desirable. Unfortunately the reality is not like this due to a phenomenon called "aliasing". Considering sinusoidal mode shapes, the issue is that some pairwise modes (like mode 29 and 31) can not be distinguished by their samples as the mode shapes will look identical (except for the sign). A more specific example of this can be found in Lie & Kaasen [2006]. Summarized, this means that there are two options for inserting mode shapes in the $\boldsymbol{\varphi}$-matrix:

1. All available modes up to the number of measurement-points (N=M) are considered.
2. Only modes that are likely to be present according to prior judgement, but not with a number higher than the number of measurement-points (N<M), are considered.

In general, a system with fewer modes than the possible maximum will give a more reliable result as the degree of estimation errors is reduced.

The mode shapes are found by either using computer programs like RIFLEX or by using sinusoidal mode shapes, which for some tests has shown to give nearly identical results, ref Lie & Kaasen [2006]. Using sinusoidal shapes, the model should have uniform tension along its length. The sinusoidal mode shapes are formulated like this:

$$\varphi_n(x) = sin\frac{n\pi}{L}x \tag{2.5}$$

Where n is the mode number, x is the coordinate along the structure and L the length of the structure.

An important issue with this modal analysis is that "noise", incorrect measurements, needs to be considered as it may prevent identification of modes. Even though a filtering is performed before such analyses is done there will most likely be some measurements that are incorrect. An error analysis of the calculated modal weights should therefore be executed. An example of this is described in Lie & Kaasen [2006].

When having obtained all weight factors for all the considered modes in the specified time interval, it is useful to calculate the RMS-values to see which modes dominate in each test case. But it is also of interest to plot all the weight factors for all modes with time. Then one can study how each mode vary in the participation of the global deformation, which is another good way of learning how a structure in VIV-condition behaves. It is also of interest to study the mode-behaviour together with the frequency interaction. This is because experiments have shown that modes seems to change from one to another, while the frequency is the same. Maybe will some cases also show that frequency changes while the mode remains constant. These aspects are of interest to be studied further as prediction of this type of behaviour is not possible by existing methods (ref Larsen [2012]).

Instead of using only one set of measurements, as in the method described above, it is an option to do a combined analysis for instance by using both acceleration and strain measurements. This provides opportunities for including more modes in the analysis. Such a combined analysis is done for the same test as being investigating in this thesis, the NDP-test programme of a riser in different current states. A detailed description is found in the report Kristiansen & Lie [2005].

Chapter 3

The VIVANA approach

VIVANA is a computer program that can calculate response on a slender structure due to VIV conditions. It is developed by MARINTEK and NTNU, and is a common used tool for oil- and engineering companies dealing with such structures. In short VIVANA can be summarized as follows:

1. First step is to identify the actual response frequencies out of all possible response frequencies. The actual active frequencies are then ranked to determine which frequency (or frequencies) that dominate.
2. Secondly the dynamic response corresponding to each of the dominating frequencies are determined. The complex frequency response method is used in this context.
3. The last step is to use all response results to find fatigue damage on the structure. Two assumptions may be used when relating the found responses to the structure. One is the space sharing approach, where response frequencies act simultaneously, but each at different points along the structure. The other approach is time sharing, where one frequency dominate the entire structure for a period of time, until another frequency takes over.

The most interesting part of the analysis in VIVANA *for this thesis* is step one, where the response frequencies are chosen, and also how frequencies are predicted to interact. This part is suspected to include too many, or not the correct, active frequencies, and it is also a time-consuming part of the analysis. Consequently it is of key interest to improve this part of the program which obviously will also improve and give more accurate results for the fatigue damage calculations. Improvement may be obtained by processing measurements in different ways, providing new and more accurate information of how the frequencies actually interact and of other parts of the analysis that can be improved. To be able to compare findings from experiments with the methods in VIVANA a more detailed description of the first step is necessary as a base for further investigation.

3.1 Determination of possible response frequencies

After a static analysis of the modelled riser is performed in the riser analysis package RIFLEX, an initial eigenvalue analysis is executed. The result is a number of mode shapes and corresponding eigenfrequencies, which is supposed to cover a range including all possible active response frequencies.

The eigenvalue analysis is performed by applying added mass for the riser in *still water* (user input). However, under actual VIV conditions the riser will have a different added mass, and the calculated eigenfrequencies can not be taken as the correct response frequencies. Hence, an iteration is carried out for a subset of the initially calculated eigenfrequencies to find a set of actual response frequency candidates containing an updated added mass. For each possibly active eigenfrequency an iteration is performed as explained in the following steps (based on Larsen [2010] and Larsen [2012]):

1.

As initial condition (k=0) it is assumed that the actual response frequency is equal to the eigenfrequency: $f^k_{osc,i} = f_{0i}$, where k=iteration step (For $k > 0$: $f^k_{osc,i} \neq f_{0i}$).

2.

Next the non-dimensional frequency is calculated along the riser:

$$\hat{f}^k_i(z) = \frac{f^k_{osc,i} D(z)}{U(z)} \tag{3.1}$$

D(z) and U(z) is diameter and flow velocity at position z along the riser, respectively.

3.

From the non-dimensional frequencies one can find the corresponding added mass coefficients along the structure, by using the following added mass curve:

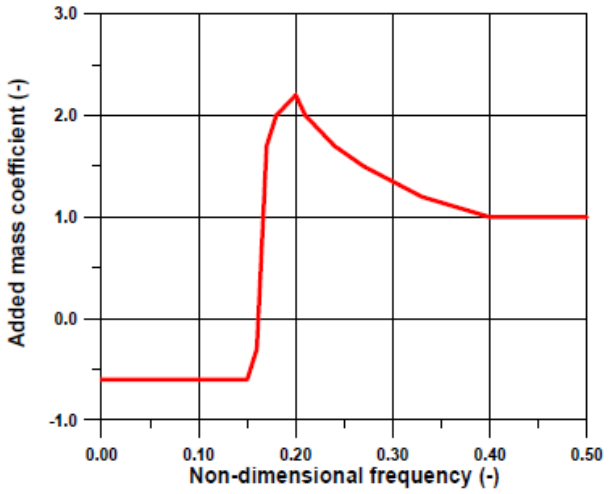

Figure 3.1: The added mass curve used in VIVANA, based on data from Gopalkrishnan [1993].

This curve is based on a contour plot of the added mass coefficient as function of amplitude and non-dimensional frequency, made by R. Gopalkrishnan (Gopalkrishnan [1993]) from forced oscillation tests with pure cross flow motions and relatively low Reynolds number. As shown in Figure 3.2, the curve in VIVANA is taken from the contour plot for a constant amplitude of 0.5D. This is a simplification, but can be done as it is seen that the curves for the added mass coefficient are close to vertical (parallel) and hence the amplitude ratio,A/D, is a less significant parameter than the non-dimensional frequency.

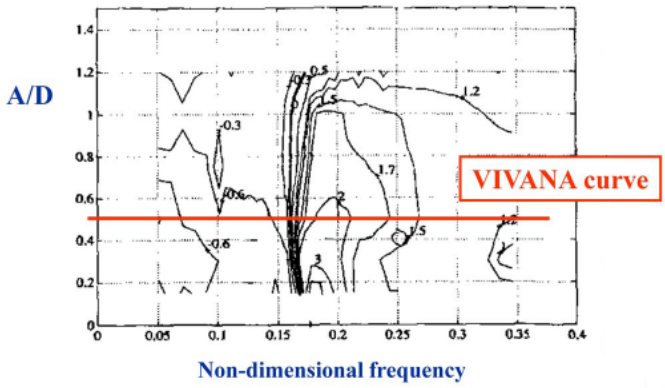

Figure 3.2: Contour plot of added mass coefficient as function of amplitude ratio and non-dimensional frequency, from Gopalkrishnan [1993]. The orange line indicates the basis for the added mass curve used in VIVANA analysis

4.

After having found new values for added mass, the mass matrices can be updated, and a new eigenfrequency, f_{0i}^{k+1} can be calculated from this. The new eigenfrequency is compared to the old one and if they are close enough, convergence is obtained. In other words convergence in this case means that there is consistency between local non-dimensional frequency, added mass and eigenfrequency. If convergence is not obtained, another iteration is needed. However, if the new eigenfrequency is satisfactory, this is accepted as a possible response frequency.

This iteration needs to be done for all eigenfrequencies that may represent a possible response frequency. As one may suspect from reading the description of the iteration for finding correct added mass, this is a demanding part of the computer program. It will therefore be an important development for VIVANA if it is possible to simplify this iteration, which may be done by studying the added mass for VIV-cases performed in model tests.

When all the necessary iterations for obtaining consistency between added mass and eigenfrequency are done, the next step is to calculate the non-dimensional frequency along the structure for these frequency candidates. Those that are observed to have a zone along the structure with non-dimensional frequency between 0.125 and 0.3 are taken to be actual excitation frequencies. The reason for selecting the candidates within this range of non-dimensional frequency is seen from another contour plot by Gopalkrishnan, see Figure 3.3.

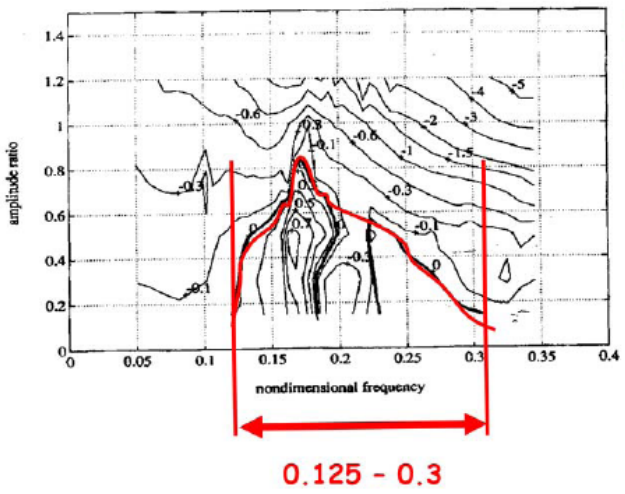

Figure 3.3: Contour map of the excitation force coefficient against amplitude ratio and non-dimensional frequency. Red part indicating excitation range. From Gopalkrishnan [1993].

The plot shows a contour map of the excitation force coefficient, C_e, as function of amplitude ratio and non-dimensional frequency. The red part indicates where C_e is positive and is taken as the excitation range, and hence this is used as a criteria for choosing frequencies that will actually participate to excite the riser.

3.2 Choice of dominating frequency

The approach by choosing frequencies within the mentioned excitation range will make several response frequencies overlap each others excitation zones along the riser, but in reality one zone can have vortex shedding at only one frequency at a time. Therefore these response frequencies needs to be ranked in order to decide which one will dominate.

This is done by introducing an energy criteria in the shape of the following integral:

$$\int_{L_E} U^3(z)D^2(z)(\frac{A}{D})_{C_{e,CF}=0}dz \tag{3.2}$$

$(\frac{A}{D})_{C_{e,CF}=0}$ is the non-dimensional amplitude that gives zero dynamic lift force (excitation force, cross-flow), U is the flow velocity, D the diameter and L_E the length of the excitation zone.

The one frequency in a zone which has the largest value of this integral is taken as the dominating frequency. However, since it is stated that all the frequencies within the mentioned interval of non-dimensional frequency somehow participates in the excitation of the riser, an interaction between them is necessary.

One approach is most easily shown with a structure in linearly sheared current. The dominating frequency in this approach will excite the riser along its entire excitation zone, while the rest of the active frequencies will excite the remaining parts of the structure. The procedure is best shown with a figure:

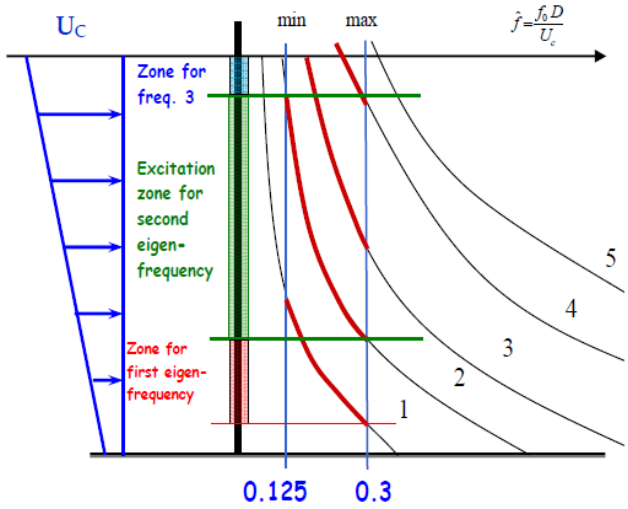

Figure 3.4: Several possible response frequencies, expressed by non-dimensional frequency along a riser in sheared current. Four of the frequencies are within the excitation range. Figure from Larsen [2012].

This is an example where four of the possible response frequencies lies within the excitation range. The second frequency is found to be the dominating one, and hence controlling its entire zone. Frequency one and three controls the rest of the riser. This is known as concurrent response frequencies, or space sharing, as described briefly in the introduction (chapter 1). It is also important to mention that when calculating responses from this condition, one part at a time is considered as an excitation zone, while the parts outside this zone are taken as damping zones.

Another approach for interaction between active response frequencies is best shown by a case in uniform current. As the current velocity is the same all over the structure for this case, the picture of non-dimensional frequency along the length will look slightly different. Figure 3.5 shows this case.

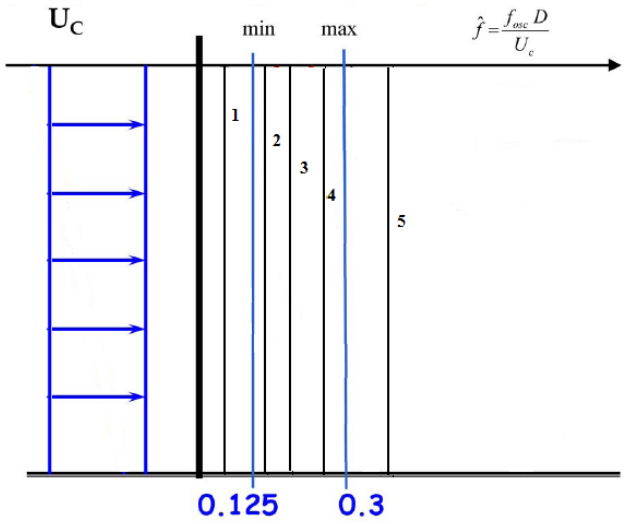

Figure 3.5: Several possible response frequencies, expressed by non-dimensional frequency along a riser in uniform current. Three of the frequencies are within the excitation range.

In this case a non-dimensional frequency does not vary along the riser, and therefore the one frequency with largest value of the energy criteria will dominate the entire length of the riser, but only for some time. The other active frequencies will get their share of time to excite the structure, but the dominating one gets the longest period. This condition is known as consecutive response frequencies, or time sharing, as briefly described in the introduction (chapter 1).

For uniform current, the two first terms in the integral, equation 3.2, will be identical for two response frequencies. Therefore, the last term $(\frac{A}{D})_{C_{e,CF}=0}$ is especially important for this kind of cases. The way VIVANA predicts/finds this value is once again mainly based on data found by Gopalkrishnan. The same contour plot as used for defining the excitation range is also used as a basis for drawing curves with excitation force coefficient as function of non-dimensional amplitude, for different non-dimensional frequencies. As seen to the right in Figure 3.6, the three points, A, B and C, define parts of the graphical picture, while the curve *between the points* is made by two second order polynomials. The values in point A and B are found from the curve of Gopalkrishnan, but $(\frac{A}{D})_{C_{e,CF}=0}$ in point C is a compromise between Gopalkrishnans results and results from a PhD thesis by K. Vikestad, Vikestad [1998]. Figure 3.6 is showing the mentioned curve and how it is partly based on the contour plot of Gopalkrishnan.

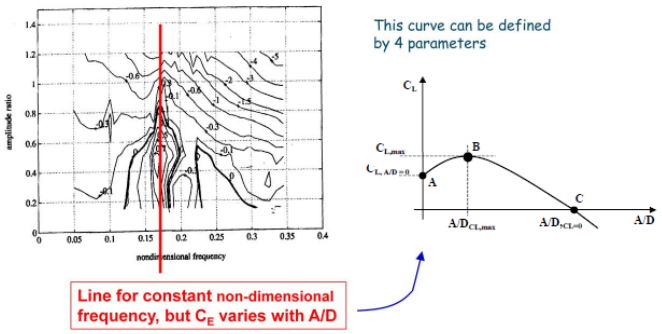

Figure 3.6: Contour plot by Gopalkrishnan to the left, showing how values are found for one non-dimensional frequency. To the right; Excitation-/liftcoefficient curve based on the plot to the left and results from Vikestad [1998]. Figures from Gopalkrishnan [1993] and Larsen [2012].

The curve to the right on Figure 3.6, can be made for all desired non-dimensional frequencies. VIVANA make such curves from a modified parameter plot, instead of directly using Gopalkrishnans contour plot. This parameter plot is shown in Figure 3.7.

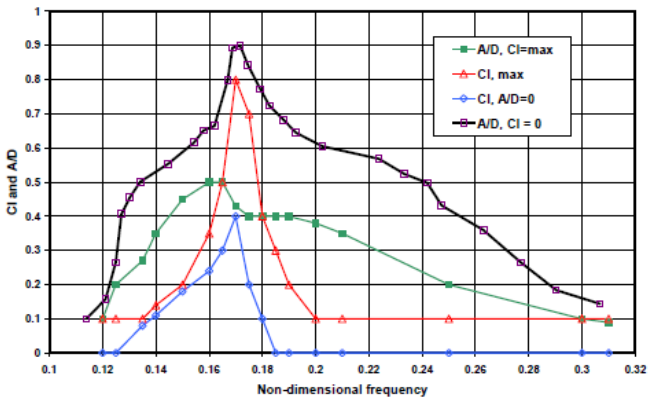

Figure 3.7: Curves defining the parameters to be used for generating dynamic lift coefficient curves in VIVANA. From Larsen [2010].

From this plot the value of $(\frac{A}{D})_{C_{e,CF}=0}$ can be found for all desired non-dimensional frequencies.

Chapter 4

Methods used for analysing the NDP testdata

As explained in the introduction, an analysis in MATLAB of one of the tests executed through the Norwegian Deepwater Programme (NDP), was done in the project thesis (Brunborg [2012]). The goal was to look at the dominating oscillation frequencies regarding VIV of the tested riser, to see if one were able to see a pattern throughout time or along the length of the riser. To be able to verify a pattern it is necessary to look at several time series, with different velocity and profile for the current. So by only looking at one test result in the project thesis it was not possible to draw any conclusions or to see a pattern. However, the knowledge gained on execution of the analysis is a great achievement that is utilized in this thesis to accomplish a more detailed and organized investigation. This chapter explains the methods used.

4.1 About the NDP-test

The test is a "High Mode VIV Test" on a modelled riser with a large length-to-diameter (L/D) ratio, carried out for the Norwegian Deepwater Programme. The riser was 38m long, made of fiberglass with an outer diameter of 27mm and a wall thickness of 3mm. It was set up horizontally and towed in ways simulating both uniform and sheared current, and with different velocities. It was tested both with and without VIV-suppression devices, but this thesis only comprises the test results of a bare riser without any strakes.

To measure the bending strain, which is the raw data used as basis in this thesis, 24 strain gauges for CF results and 40 for IL results were located along the riser. In addition, 8 accelerometers were also part of the instruments on the riser. The instrumentations saved 1200 signals per second (meaning sampling frequency = 1200Hz). In this thesis, only cross-flow is considered.

More details of the set-up and execution of this test programme can be found

in Braaten & Lie [2012]. A good description and discussion of results are also performed in Trim et al. [2005].

4.2 Use of strain versus displacement values.

As mentioned, the raw signals measured in the NDP-test is strain, which is what all results and plots in this thesis are based upon. Using strain instead of displacement as basis for investigation implies that some aspect must be kept in mind when interpreting the results.

Strain, presented by curvature, is the second spatial derivative of the displacement mode shape. This means that the strain (curvature) is related to the displacement by the mode number squared, since for a sinusoidal mode shape

$$\phi(z) = asin(n\pi z/L) \tag{4.1}$$

with amplitude a, the curvature becomes:

$$\phi(z) = -a(n\pi/L)^2 sin(n\pi z/L) \tag{4.2}$$

The difference to be aware of is shown when comparing two mode shapes for displacement and two for curvature, with the same amplitude. Sinusoidal modes one and two for displacement is expressed below:

$$\phi_1(z) = asin(\pi z/L) \tag{4.3}$$

$$\phi_2(z) = asin(2\pi z/L) \tag{4.4}$$

while the two first modes for strain (curvature) is:

$$\phi_{1,xx}(z) = -a(\pi/L)^2 sin(\pi z/L) \tag{4.5}$$

$$\phi_{2,xx}(z) = -a(2\pi/L)^2 sin(2\pi z/L) \tag{4.6}$$

This shows that for strain, the absolute values increase more from one mode to another compared to displacement values. In the example above, the curvature for mode one will be 1/4 of the curvature of mode two if they have the same amplitude.

Making amplitude plots from displacement values would be the best for studying and seeing the oscillations directly, but from amplitude plots one is also able to see approximately which mode that will dominate, which was described in section 2.2. And since dominating modes for strain (curvature) indicates which mode that

will give the largest contribution to bending stresses, the use of strain as basis in this thesis can actually be preferable as results shall be compared with VIVANA, which predicts fatigue damage.

4.3 Frequency plots

The first task performed in this thesis was generating the type of frequency plot as mentioned in section 2.1. This is the same type of plot as generated in the project thesis (Brunborg [2012]), only now it is done for a lot more cases. Analyses are performed of ten cases where the riser is exposed to uniform current profile with velocities from 0.5 m/s up to 2.4 m/s. In addition, ten cases with a linearly sheared current profile with velocities also from 0.5 to 2.4 m/s, are analysed. A full overview of the cases and corresponding towing/current velocities is found in table C.3 in appendix C. As concluded in Brunborg [2012], cases with higher velocities are expected to show more variation in dominating frequencies than the one case studied there. Higher velocities implies that the riser will move with modes of higher order. And with high modes, the dominating frequencies change more easily from one to another, making these kind of cases interesting as interaction between frequencies are to be studied. This is explained in more detail and shown with a figure in [Brunborg, 2012, p. 24]

To be able to generate the plots that show dominating frequencies of the riser deflection due to the VIV, the time series with measured strain signals along the riser needs to be decomposed into the time-frequency space. In this case it is used a Wavelet analysis to do this. A brief discussion of Wavelet in relation to this work is done in [Brunborg, 2012, p. 19], but the details behind the method is found in other literature such as [Grossmann & Morlet, 1984]. The codes used in MATLAB for doing this is provided by Jie Wu (MARINTEK), but some adjustments are made for fitting it to the cases used in this thesis.

In addition to go through a wavelet analysis the raw signals also needs to be filtered, both with regard to time and to levels of frequency. Since the data to be used are generated from a model test, the signals at start and end of the measuring time, where the velocity is not constant, needs to be neglected. But also a part of the beginning of the constant velocity period needs to be cut off, due to the domination of transient signals here. This is described in more detail in section "8.2.1 Time-window" in [Braaten & Lie, 2012, p. 20]. The relevant time interval to use for each case is given in files distributed from the test, so the start and end values can be read directly into the scripts in MATLAB.

Filtering of frequencies

When it comes to filtering of frequencies, the response frequencies of the riser which is closest to the Strouhal frequency are chosen.

$$f_{st} = \frac{StU}{D} \tag{4.7}$$

This kind of filtering is done by band-pass filtering, which involve fast-fourier transformation. This way the signals, which are originally in time-domain, are transformed into frequency-domain, filtered with the upper and lower limits around the Strouhal frequency, and transformed back into strain values in time-domain. This is done before the values goes through a wavelet-analysis. For more details, see the description of how the frequency range for test no. 2030 was chosen in [Brunborg, 2012, p. 21-22].

The conclusion after analysing test 2030 in the project thesis was that this case had too low current velocity, hence too low mode, to be able to see any significant changes in the dominating frequency. But at the start of the work for this thesis it was decided to filter out more frequencies from this plot, as it showed one small spot with a much higher frequency value than elsewhere. And when this was done, the picture suddenly looked quite different. The small spot was most likely an error in the measurements or a transient value not filtered out, contributing to a "false" picture of how the frequencies really behave. The plot as it was made in the project thesis is shown in Figure 4.1, while the new plot with a more narrow frequency range is shown in Figure 4.2.

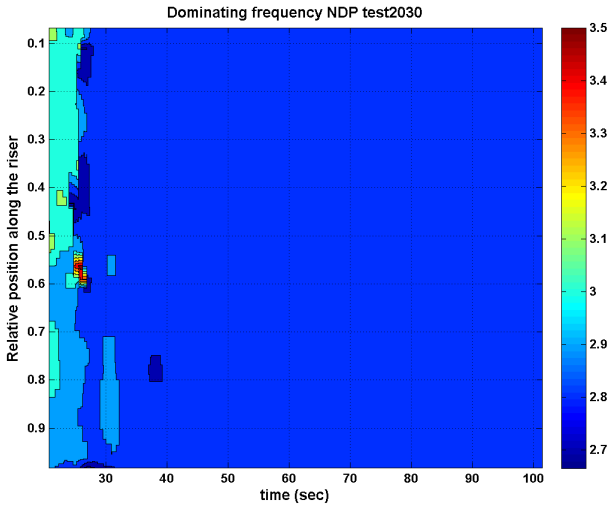

Figure 4.1: MATLAB-plot showing the variation of dominating frequencies in both time and along the riser, as presented in the project thesis, Brunborg [2012].

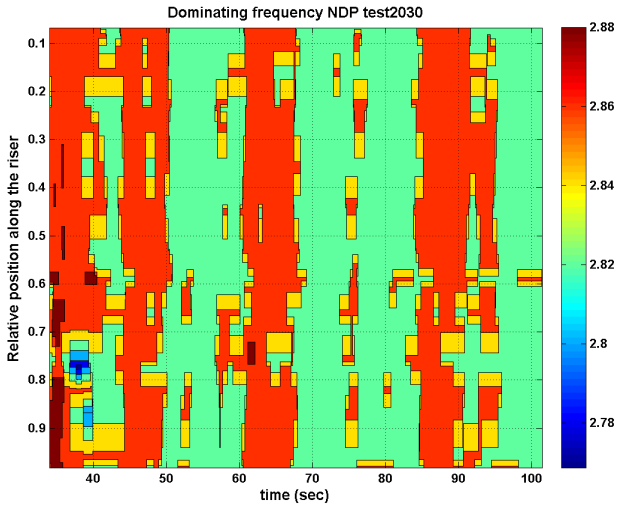

Figure 4.2: MATLAB-plot showing the variation of dominating frequencies in both time and along the riser, after excluding the highest frequencies.

It is clear that the frequency has more variation in Figure 4.2 than in Figure 4.1, where mainly two frequencies alternate through time. This discovery meant that

when generating plots like this, one has to be more considerate when choosing the frequency range. As described in [Brunborg, 2012, p. 22] the range was originally chosen to be from $0.5f_{st}$ to $1.5f_{st}$, a broad range around the theoretical Strouhal frequency (vortex shedding frequency). This is a good starting point, but in order to get the best possible frequency picture, the 20 mentioned cases in this thesis were analysed twice. First the frequency plots were made by using the frequency range $0.5f_{st}$ to $1.5f_{st}$, then these plots were studied to see which frequency range should really be used in order to get a more detailed picture. Secondly, a new analysis with the found frequency range was performed. The final frequency plots are commented and discussed in chapter 5.

4.4 Amplitude plots

As mentioned in section 2.2, amplitude plots of either the strain or the displacement can for instance be used to show the behaviour of a structure in VIV-condition in matter of standing/travelling oscillating pattern and dominating mode order. Mainly, these plots ended up being used for finding the mode order, for further use in calculation of actual added mass.

For generating these plots it is used codes in MATLAB developed by Jie Wu (MARINTEK) as a basis. The codes start by taking in the raw signals and the needed parameters (from files distributed from the NDP-test). From this the signals are filtered with regard to both time and frequency, as for the frequency plots explained in the previous section. The time filtering is done to avoid transients and to gain a time series at constant velocity. The filtering of frequencies is the same as explained for making the frequency plots. It is first developed a plot where frequencies outside the range $0.5f_{st}$ to $1.5f_{st}$ are excluded, and from this plot a new frequency range may be found to make a second, more detailed frequency picture.

These plots are also made for each of the 20 cases that was to be investigated. As opposed to generating frequency plots, where the raw strain signals needed to be transformed with a Wavelet-analysis, the raw signals are used directly in the amplitude plots. As the raw measurements in the NDP test-programme is strain, it is the strain amplitudes and not the displacement amplitudes that are plotted, as discussed previously.

To estimate the mode from this type of plot, one has to do a "counting" of either the tops or bottoms, as only cross-flow is considered. In Figure 4.3, this means counting the dark or light "rows". As an extra tool for counting the mode order it is also made "surface"-plots (of the same strain values) for some of the cases where it was difficult to estimate the mode from the regular plots. Here, the mode order can be found by counting only the "top-peaks" (or only the "bottom-peaks"), as can be seen in Figure 4.4.

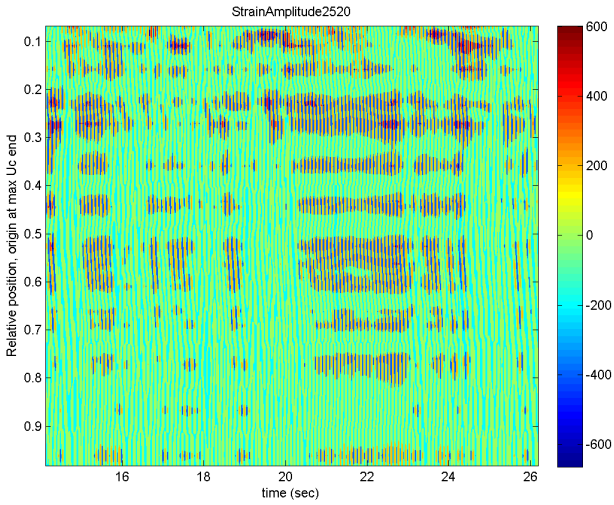

Figure 4.3: Example of strain amplitude plot, for a riser in sheared current of max velocity (in origin) 2.4 m/s. It seems as the dominating mode is approximately 12-13.

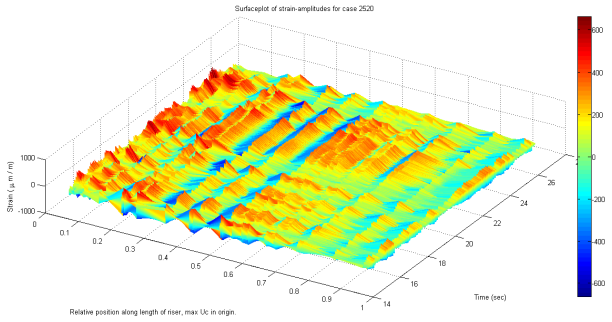

Figure 4.4: This surface-plot can be used as a supplement to the one in Figure 4.3, for verifying the mode. Mode 12-13 seems quite right, although it is not all clear in this plot either.

As can be seen in the Figures 4.3 and 4.4 it is not so easy to find the exact dominating mode order, but an approximate mode number can easily be found. All results are commented in chapter 5, where the mode order found from these plots are used as an important basis.

4.5 Added mass calculations

As mentioned in the theory of VIVANA, chapter 3, it would be a good achievement if the iteration related to finding consistency between added mass and eigenfrequency can be simplified. With this in mind it is of interest to obtain information regarding the behaviour of actual added mass. Therefore it is performed calculations of added mass from the NDP-test results, to see if a trend can be observed.

From courses covering theory of marine dynamics it is known that for obtaining the eigenfrequency of a beam with tension, which represents slender marine structures, one combines the formulas for eigenfrequency for a *string with tension* and a *beam without tension*. The equations are shown below.

Eigenfrequency for string with tension:

$$\omega_S = \frac{n\pi}{l}\sqrt{\frac{T}{m+m_A}} \tag{4.8}$$

n is the mode number, l is the length [m] of the string, T the tension [N], m the mass [kg/m] of the string and m_A the added mass [kg/m].

Eigenfrequency for beam without tension:

$$\omega_B = \frac{n^2\pi^2}{l^2}\sqrt{\frac{EI}{m+m_A}} \tag{4.9}$$

n is the mode number, l is the length of the beam, EI is the bending stiffness $[Nm^2]$ of the beam, m the mass of the beam and m_A the added mass.

Since the mode shapes of the string and the beam are identical, the stiffness of a beam with tension will be the sum of the stiffness of the two cases above. The eigenfrequencies above can be written as

$$\omega_S = \sqrt{\frac{k_S}{m+m_A}} \tag{4.10}$$

k_S is the stiffness of the string with tension.

$$\omega_B = \sqrt{\frac{k_B}{m+m_A}} \tag{4.11}$$

k_B is the stiffness of the beam without tension.

And the stiffness of the beam with tension is the sum:

$$k_{BS} = k_S + k_B \tag{4.12}$$

From this the eigenfrequency for the beam with tension can be written as:

$$\omega_{BS} = \sqrt{\frac{k_{BS}}{m + m_A}} = \sqrt{\frac{k_S + k_B}{m + m_A}} = \sqrt{\omega_S^2 + \omega_B^2} \tag{4.13}$$

Introducing equations 4.8 and 4.9 into 4.13 the eigenfrequency for a beam with tension, representing eigenfrequency for slender marine structures, becomes:

$$\omega_{BS} = \frac{n\pi}{l}\sqrt{\frac{T}{m + m_A} + (\frac{n^2\pi^2}{l^2} * \frac{EI}{m + m_A})} \tag{4.14}$$

Then this equation is transformed to give an expression for the added mass, m_A:

$$m_A = \frac{T + \frac{n^2\pi^2 EI}{l^2}}{(\frac{\omega_{BS} l}{n\pi})^2} - m \tag{4.15}$$

Further, the added mass for each case are found from this. The tension-values for each case was distributed by supervisor Carl Martin Larsen, and the values are seen in table C.1 in appendix C together with the rest of the calculations and parameters used. The mode number used for each case are found from the strain amplitude plots, as mentioned in the previous section, and are approximate values. The "eigenfrequency", ω_{BS}, to be entered into the equation is taken as the average of the min and max values in the generated frequency plots. The mass for the riser is taken from Braaten & Lie [2012] and is the mass of waterfilled riser. The bending stiffness, EI, is distributed from Prof. Carl Martin Larsen as the value for EI in Braaten & Lie [2012] is found to be incorrect.

The obtained values for added mass for all cases are plotted together with the dominating modes in MATLAB to be studied.

Chapter 5

Results and observations

This chapter includes comments and discussions in relation to the results obtained from the methods described in the previous chapter. The cases with uniform current and sheared current are first discussed separately and then compared, in addition to other observations.

5.1 Uniform current cases

As mentioned in the previous, it is generated both frequency and amplitude plots. From that it is of interest to look for trends in how the riser behaves, with a goal of improving computer programs like VIVANA.

Frequency interaction

First of all the goal was to look for a pattern regarding space- and time sharing. For studying this it was expected to be of most interest to look at the frequency plots indicating how the oscillating frequency of the riser changes in space and time. Ten cases with uniform current were analysed, and all the resulting plots can be found in section A.1 in appendix A. From these plots one can see that the dominating frequencies does not tend to have a clear pattern, neither in time development for one case, nor with increasing current velocity in general. However, some cases do have some interesting parts of the time series. For instance, case 2120 has periods where one frequency seems to control the entire riser, see Figure 5.1 below.

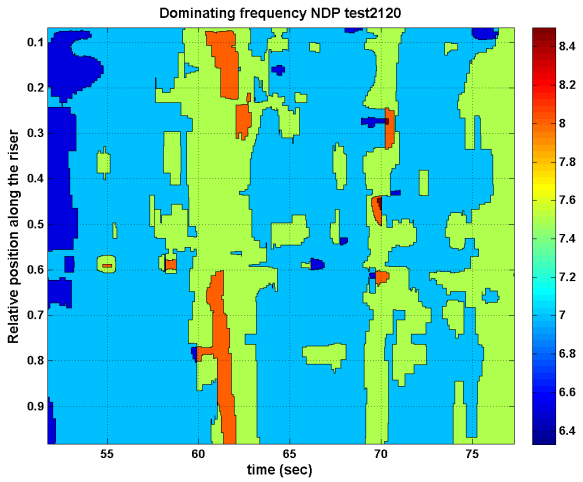

Figure 5.1: Dominating frequencies for case 2120, velocity of current is 1.4m/s. In some periods, one frequency tends to control the entire riser.

The light blue colour, corresponding to a frequency of 7 Hz, seems to be controlling more or less the entire structure for some periods of time. The green colour, corresponding to approximately 7.5 Hz, dominate significant parts of the riser the rest of the time. This can be seen as a small sign of time sharing, but in general in all other uniform current cases the frequency-interaction looks more like a mixture of time- and space sharing. Indication of time sharing is found to be slightly more clear in the sheared current cases, discussed in the next section.

Strain amplitudes

The other type of plot generated is the amplitude plot for strain. For the same ten cases in uniform current, these plots are presented in section B.1 in appendix B. Also these plots show a somehow disorderly picture, which is not so easy to draw any conclusions from. As written in section 2.2 such plots may be used to identify cases of interest in relation to further statistical studying of the amplitudes. This has however been found to be a bit difficult from the generated plots, and it was decided not to focus any further on this particular approach.

However, the amplitude plots can be used to identify which mode of strain is dominating for each of the cases, as mentioned earlier. In this thesis, dominating mode of strain is important information because it is used for determining added mass, which is discussed in section 5.4. The subjective choice of dominating strain mode, as described in section 4.4, may be an uncertainty in the calculations of added mass. Hence a verification of the dominating strain modes are performed.

This was possible to do as a modal analysis was executed of the NDP-measurements and documented in Kristiansen & Lie [2005]. The modal analysis was done for both curvature and acceleration separately and in a combined approach. It is the results of dominating curvature modes from Kristiansen & Lie [2005], which is used as verification for the findings of dominating strain modes. Figures 5.2 and 5.3 shows the dominating modes for curvature from Kristiansen & Lie [2005] and the dominating modes for strain from this thesis, respectively. The figures applies to uniform current and current velocities (towing velocities) up to 2.5 m/s.

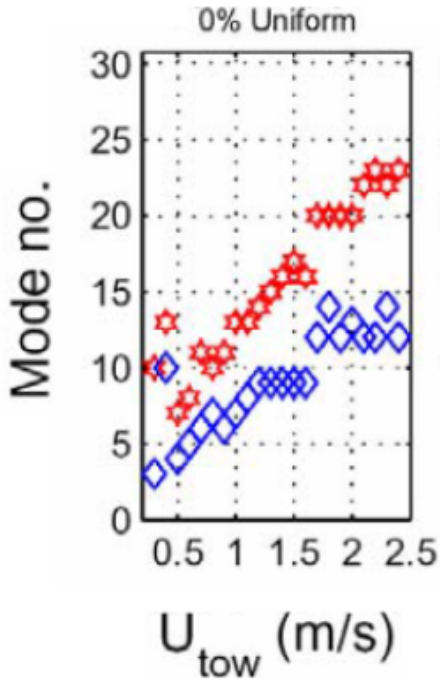

Figure 5.2: Dominating modes for curvature, for bare riser in uniform current. Red markers = IL, blue markers = CF. Figure from Kristiansen & Lie [2005].

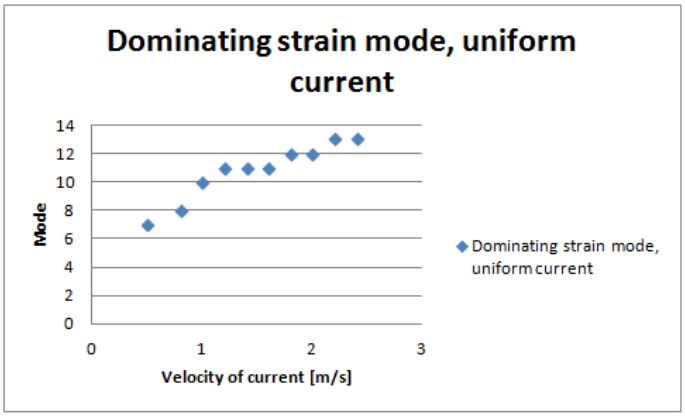

Figure 5.3: Dominating modes for strain in CF, for bare riser in uniform current.

The modes found from the generated amplitude plots for strain in this thesis are seen to be lying between mode 6 and 14, for current velocities between 0.5 and 2.5 m/s. The modes for curvature from the modal analysis seems to be lying between 4 and 15 for current velocities (towing vel.) from 0.5 to 2.5m/s (blue markers indicate CF, which is relevant here). Since curvature is just a different presentation of strain, this provides a good verification that the found strain modes in this thesis are usable and reliable values.

5.2 Sheared current cases

The same type of plots as generated for uniform current are also made for the ten sheared current cases; frequency plots and amplitude plots.

Frequency interaction

The plots with dominating frequencies, which are gathered in section A.2 in appendix A, more or less give the same impression as for the uniform current cases at first sight. However, a more comprehensive study reveals that it may seem to be slightly more order than for the uniform current cases. Some frequencies tend to dominate both at a longer time interval and in higher degree along the entire structure. The latter is a bit strange as it is the cases with uniform current that are expected to have more or less one frequency dominating the entire length. Looking at the frequency plot of case 2460, Figure 5.4, one can see a good example of a frequency that both dominates the entire length of the riser and at a quite long period of the time.

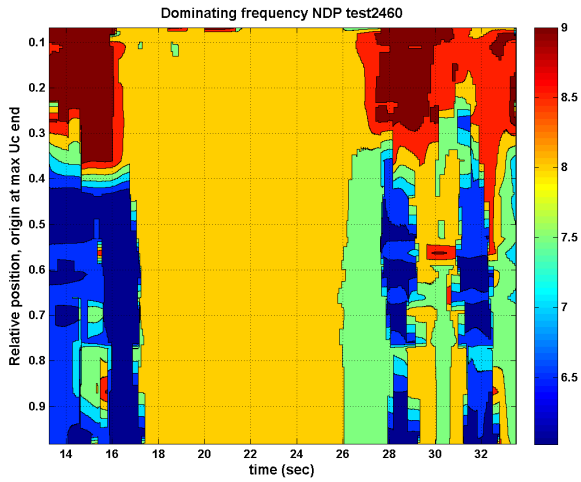

Figure 5.4: Dominating frequencies for case 2460, max velocity of current is 1.8m/s. One frequency seems to dominate the complete riser in some period of time.

The entire riser in case 2460 seems to be controlled by a frequency of 8 Hz, for about 8 seconds. The rest of the time, the picture is much more chaotic.

More of the cases in sheared current can be seen to have similar behaviour as case 2460 for some periods of time, but in general it seems to be some kind of mix of space- and time sharing, as for the uniform current cases. In other words it is not easy to draw any conclusions other than that the reality of VIV is complex and not easy to predict.

Degree of participation in time for active frequencies

Another way of presenting the results for active frequencies is to look at the total time-occupancy for each frequency at one specific position along the riser. This statistics will give a good picture of which frequencies are dominating at this point. A figure containing this information of all the ten cases of sheared current are shown below in Figure 5.5. The position used for all cases is the place where the current is $2/3U_{max}$.

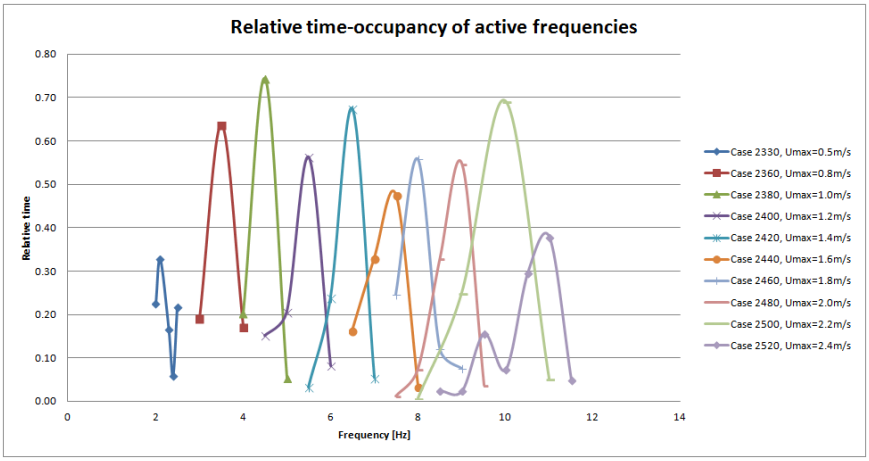

Figure 5.5: The degree of participation in time for active frequencies is shown for all ten cases of sheared current at position along riser where the velocity is $2/3U_{max}$.

The values used to generate the plot in Figure 5.5 are presented in table C.2 in appendix C. This information can be used in comparison of results from VIVANA in further work, to see if the periods of dominance agree with what is seen there.

Strain amplitudes

The amplitude plots of sheared current cases are shown in section B.2 in appendix B, and looks actually quite good. However, as for the cases in uniform current, these plots are in the end only used for predicting a dominating mode to be used in calculations of added mass.

As for the uniform current cases, a verification of the modes found by "counting" the peaks in the amplitude plots are also executed for the sheared current cases. Dominating curvature modes from Kristiansen & Lie [2005] and dominating modes of strain from this thesis is shown in Figures 5.6 and 5.7, respectively.

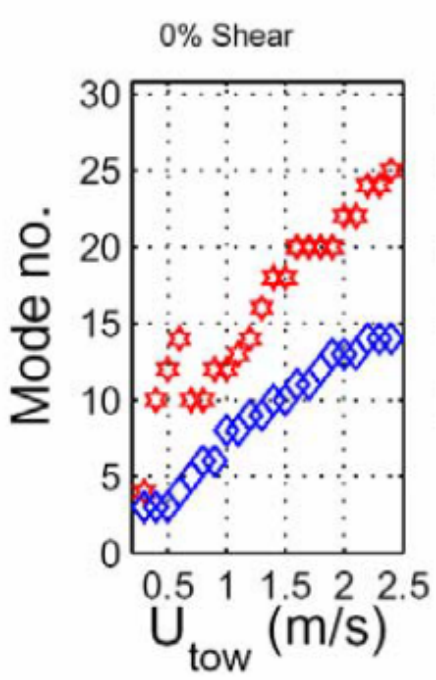

Figure 5.6: Dominating modes for curvature, for bare riser in sheared current. Red markers = IL, blue markers = CF. From Kristiansen & Lie [2005].

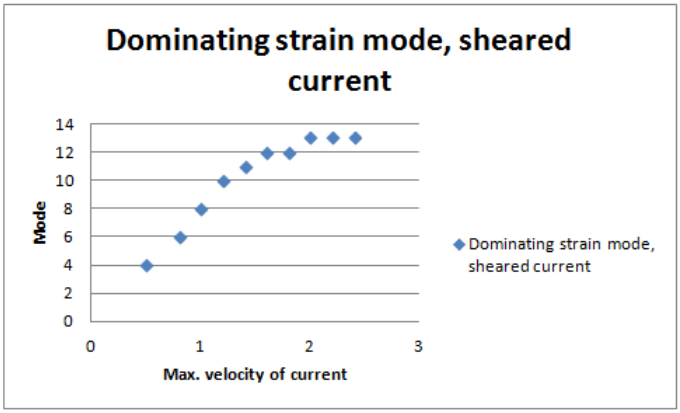

Figure 5.7: Dominating modes for strain in CF, for bare riser in sheared current.

From Figures 5.6 and 5.7 it is observed a good consistency between the results. From the modal analysis, the dominating modes for curvature seems to be lying between 4 and 15 for velocities of 0.5-2.5 m/s. (blue markers indicate CF, which is relevant here), as for the uniform current cases. The dominating modes for strain from results in this thesis seems to be lying between 4 and 14 for the same velocities. Hence, also the dominating modes found for sheared currents seems to be reliable!

5.3 Comparison of uniform and sheared current

Summarising the two latest sections; it is not easy to draw conclusions for either uniform or sheared current cases in order to systematize the behaviour of a riser in VIV-condition. But if a comparison is to be done of the two types of current, the behaviour seems to be slightly more in order for the sheared current cases than for the uniform ones. And as mentioned, this is not quite as expected as uniform current in theory should have a more clear/easy behaviour than the sheared current.

For summarising the results regarding the active frequencies, it is made a graph showing the min and max active frequencies for all cases from the obtained frequency plots, together with the Strouhal frequency (equation 4.7) and the eigenfrequencies (modes). The Strouhal frequency is found with Strouhal number of 0.17, as used in Braaten & Lie [2012], and for sheared cases the velocity used is 2/3 of U_{max}. The eigenfrequencies/modes are in this plot for displacement, and was distributed from Prof. Carl Martin Larsen. A plot like this for each of the two current profiles are shown below:

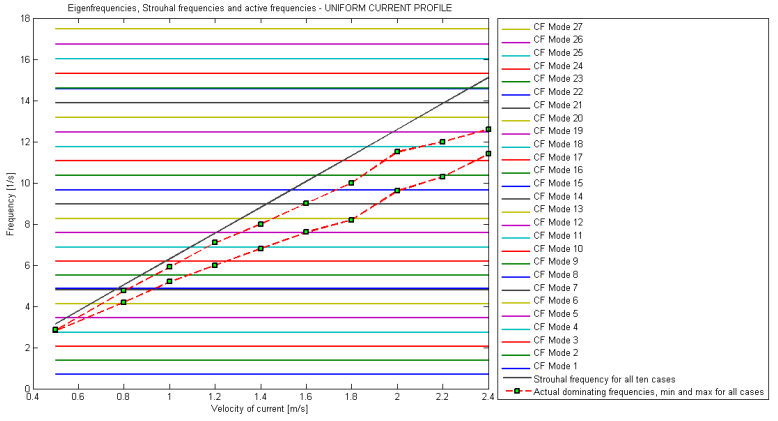

Figure 5.8: An overview of the active frequencies, eigenfrequencies and Strouhal frequency for all cases of uniform current.

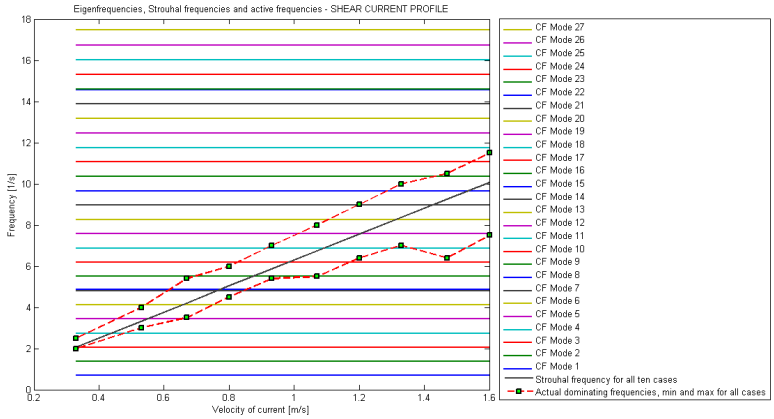

Figure 5.9: An overview of the active frequencies, eigenfrequencies and Strouhal frequency for all cases of sheared current.

From this it is seen that all the values for the active frequencies in uniform currents are lower than the theoretical Strouhal frequency, 4.7. The sheared current cases all have their min and max active frequencies on each side of the Strouhal frequency, which is logic since the Strouhal frequency is calculated by using $2/3U_{max}$. Another observation is that, especially for the sheared current cases, the bandwidth of active frequencies is expanding for higher current velocities. This may be an indication that more frequencies are active for higher modes.

5.4 Change in added mass

As explained in section 4.5 added mass was calculated from the NDP-test results for the same 20 cases as before. The obtained values for added mass are shown graphically together with the dominating strain modes for uniform and sheared current cases below in Figures 5.10 and 5.11:

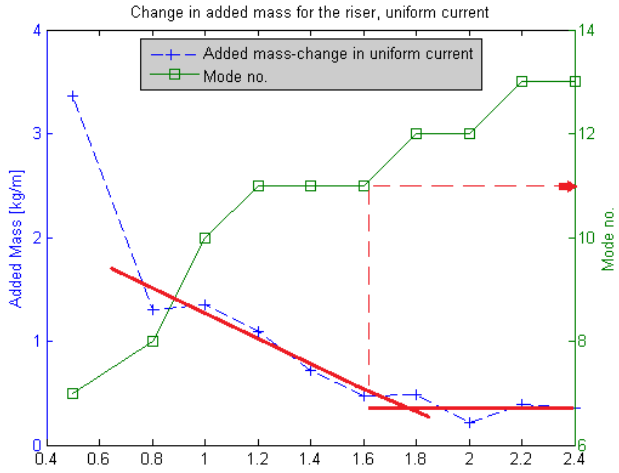

Figure 5.10: Plot of actual added mass for the NDP-riser in uniform current, with increasing current velocity. Calculations are based on observations of dominating mode and active frequencies (based on strain). Trend lines and the dominating mode for each case is also shown.

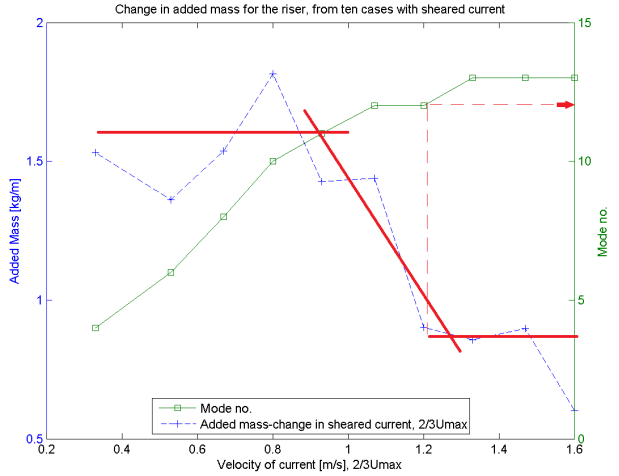

Figure 5.11: Plot of actual added mass for the NDP-riser in sheared current, with increasing current velocity. Each case is plotted against velocity=$2/3U_{max}$. Calculations are based on observations of dominating mode and active frequencies (based on strain). Trend lines and the dominating mode for each case is also shown.

These plots show the change of added mass as velocity and dominating mode

increases. It is of importance to study these when trying to gain information which can improve the iteration in VIVANA, explained in section 3.1.

What can be seen from the red trend lines drawn in Figures 5.10 and 5.11 is that, especially for the uniform current cases, the added mass seems to stabilize for cases with higher modes (higher current velocities). Of course this is based on just a small sample of cases and there might be some uncertainties related to the calculations, but it should be a good picture indicating how the added mass behaves in reality for the investigated conditions. And as shown in the previous sections 5.1 and 5.2, the values for dominating strain modes used in this calculation seems to be of good reliability, which strengthens this information.

The consequence of this observation in relation to improvement of the computer program VIVANA is that for models in current velocities/at modes higher than a certain value, the iteration done for adjusting eigenfrequency/added mass is not necessary. This is because the initial eigenvalue-analysis done for finding possible frequencies can now be inserted with a constant value of added mass, for the relevant cases, instead of the still-water values that requires an iteration. Being able to avoid iterations for several cases implies a good improvement in VIVANA as this part of the program is quite time-consuming.

From the Figures 5.10 and 5.11 it seems like the uniform current cases with velocity around 1.6m/s and higher, and approximately modes above 11, has a stable added mass somewhere around 0.4kg/m. The sheared current cases are slightly less stable, but can be seen to stabilize in some degree for cases of velocity ($2/3U_{max}$) 1.2m/s and higher, and modes approximately above 12-13, with a added mass somewhere around 0.7kg/m.

Which values of velocity and mode making the division to constant added mass is very rough, and more detailed analyses needs to be executed to find such values. But the results should be a good indication of the behaviour of added mass. And if the same observation can be found from analyses from more experiments, making it more reliable, it may be implemented in VIVANA and other similar programs where it is useful.

Chapter 6

Summary and conclusions

6.1 Conclusions

The main tasks in the description of this thesis, is to gain new information that can help describe how the response frequencies related to VIV occur in space and time. Investigation of other VIV-related parameters by studying results from experiments, is also of interest. It is desired that findings can help improve the computer program VIVANA.

To directly see any patterns for the response frequencies in time and space from the generated plots turned out to be a bit difficult. However, it can be seen signs of time- and space sharing, in some degree more for sheared currents, but not a clear pattern. This more or less confirms the conclusions from former experiments, that the real response is a combination of these two approaches.

However, when the information from the generated plots are used in calculation of added mass far more interesting results are obtained. Although the figures that show change in added mass, 5.10 and 5.11, are based on quite few cases it can be concluded that a trend is seen. The added mass seems to stabilize for vibrations of higher modes. The trend is most clearly seen for the uniform current cases, but also to some extent for sheared currents. More analyses are necessary to confirm this observation, but it is a good indication of the change in added mass for the cases studied in this thesis.

6.2 Recommendations for VIVANA

If the indication that added mass seems to stabilize for responses with higher modes can be confirmed, it will provide a basis for an important improvement in VIVANA. The iteration done for possibly active frequencies in order to ensure consistency between added mass and eigenfrequency will not be necessary for cases with high current velocities/modes, due to constant added mass for these cases.

The constant value of added mass can be inserted in the initial eigenvalue-analysis instead of the still-water-value.

6.3 Recommendations for further work

As discussed in chapter 4, some uncertainties of the methods used are related to the use of strain-signals in stead of displacement. So, considering the degree of disorder seen in generated plots, it may be a good idea to do the same analyses as in this thesis, only converting the strain to displacement-values. Especially amplitude plots of displacement would be interesting, in order to see a more direct picture of the risers behaviour.

An important aspect of further work will also be to verify and investigate further the indication of constant added mass for higher modes. This may be done by doing similar analyses as in this thesis for other experiments/model-tests. That way one can investigate structures with, for instance, other mass-ratios, and see if the same observation can be seen. It would also be of interest to study other types of currents, as only uniform and linear shear are the profiles studied in this thesis.

A fulfilment of the work in this thesis would be to carry out response analyses in VIVANA, with a riser such as the one in the NDP-test. That way one can compare results from VIVANA with respect to frequency composition with observations from this thesis. For example by looking at the participation in time of active frequencies. The energy-criteria in VIVANA deciding which frequencies dominate, can be extracted and shown together with all possible frequencies and that way see which frequencies are included and not. This may then be compared to the actual frequency-pictures found in this thesis, to see if for instance too many or too few frequencies seems to be included in the VIVANA-analysis.

Bibliography

Braaten, H., & Lie, H. 2012. *NDP Riser High Mode VIV Tests - Main Report.* MARINTEK - Norwegian Marine Technology Research Institute, Trondheim, Norway.

Brunborg, M. 2012. *Vortex Induced Vibrations of Slender Marine Structures.* Project Thesis, Department of Marine Technology, Norwegian Institute of Technology, Trondheim, Norway.

Gopalkrishnan, R. 1993. *Vortex induced forces on oscillating bluff cylinders.* PhD-thesis, Department of Ocean Engineering, Massachusetts Institute of Technology, Cambridge, MA, USA.

Grossmann, A., & Morlet, J. 1984. *Decomposition of hardy functions into square integrable wavelets of constant shape.* SIAM J.Math. Anal. - VOL.15 - No.4.

Kristiansen, T., & Lie, H. 2005. *NDP Riser High Mode VIV Tests - Modal Analysis.* MARINTEK - Norwegian Marine Technology Research Institute, Trondheim, Norway.

Larsen, C.M. 2009. *Compendium in TMR4180 - Marine Dynamics.* Department of Marine Technology - Norwegian University of Science and Technology, Trondheim, Norway.

Larsen, C.M. 2010. *Vortex Induced Vibrations (VIV) - A short and incomplete introduction to fundamental concepts.* Department of Marine Technology - Norwegian University of Science and Technology, Trondheim, Norway.

Larsen, C.M. 2012. *Vortex Induced Vibrations (VIV) - Some fundamental concepts and VIVANA theory.* Part of lecture material in the Dynamic Analysis course, Department of Marine Technology - Norwegian University of Science and Technology, Trondheim, Norway.

Larsen, C.M. 2013. *Dialogue regarding the thesis through bi-weekly meetings with supervisor.* Department of Marine Technology - Norwegian University of Science and Technology, Trondheim, Norway.

Larsen, C.M., Passano, E., & Lie, H. 2012. *Recent development of the empirical basis for prediction of vortex induced vibrations.* Article from "Hydroelasticity in Marine Technology 2012, Tokyo, Japan".

Lie, H., & Kaasen, K.E. 2006. *Modal analysis of measurements from a large-scale VIV model test of a riser in linearly sheared flow.* Journal of Fluids and Struc-

tures 22 (2006) 557-575, MARINTEK - Norwegian Marine Technology Research Institute, Trondheim, Norway.

Trim, A.D., Braaten, H., Lie, H., & Tognarelli, M.A. 2005. *Experimental investigation of vortex-induced vibration of long marine risers.* Journal of Fluids and Structures, vol. 21(2005), p. 335-361.

Vikestad, K. 1998. *Multi-frequency response of a cylinder subjected to vortex shedding and support motions.* PhD-thesis, Department of Marine Technology - Norwegian University of Science and Technology, Trondheim, Norway.

Wu, J. 2011. *Hydrodynamic Force Identification from Stochastic Vortex Induced Vibration Experiments with Slender Beams.* Doctoral thesis, Department of Marine Technology - Norwegian University of Science and Technology, Trondheim, Norway.

Appendix A

Dominating frequencies

A.1 Uniform current

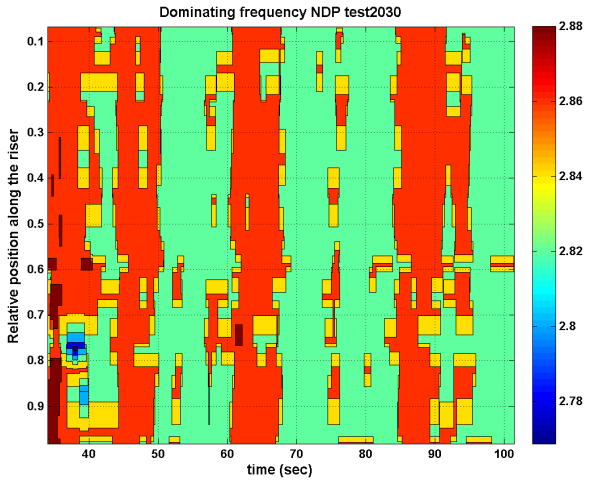

Figure A.1: Dominating frequencies for case 2030, velocity of current is 0.5m/s. Color scale on right hand side indicate the size of the frequency in [Hz]

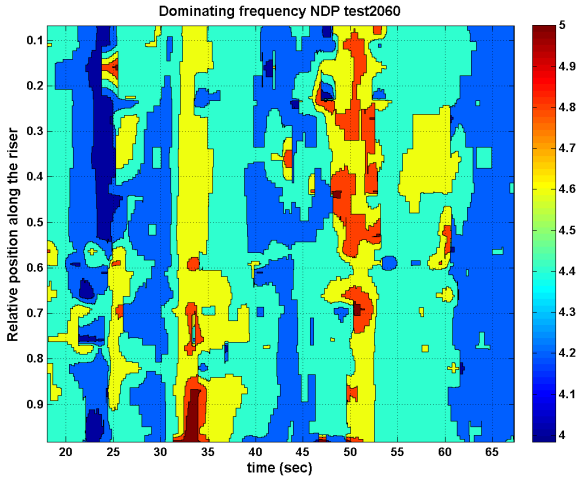

Figure A.2: Dominating frequencies for case 2060, velocity of current is 0.8m/s. Color scale on right hand side indicate the size of the frequency in [Hz]

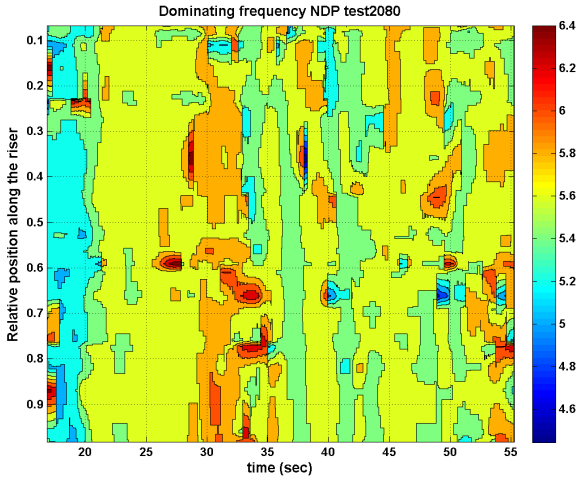

Figure A.3: Dominating frequencies for case 2080, velocity of current is 1.0m/s. Color scale on right hand side indicate the size of the frequency in [Hz]

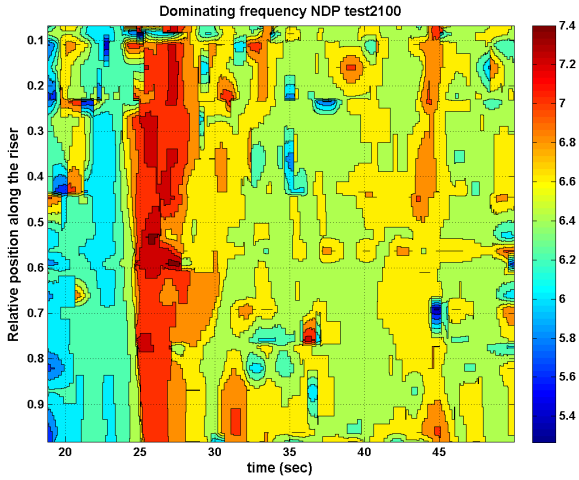

Figure A.4: Dominating frequencies for case 2100, velocity of current is 1.2m/s. Color scale on right hand side indicate the size of the frequency in [Hz]

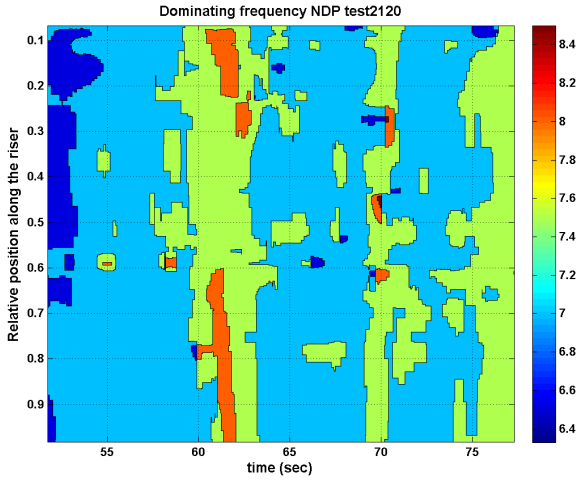

Figure A.5: Dominating frequencies for case 2120, velocity of current is 1.4m/s. Color scale on right hand side indicate the size of the frequency in [Hz]

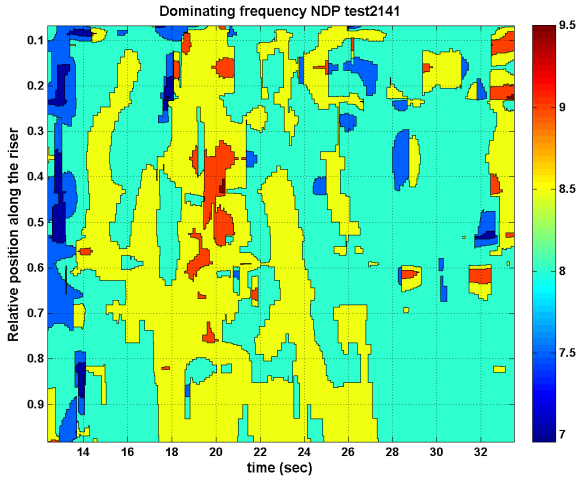

Figure A.6: Dominating frequencies for case 2141, velocity of current is 1.6m/s. Color scale on right hand side indicate the size of the frequency in [Hz]

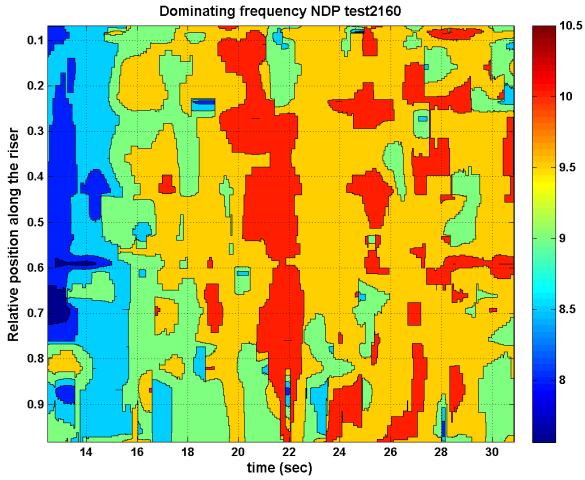

Figure A.7: Dominating frequencies for case 2160, velocity of current is 1.8m/s Color scale on right hand side indicate the size of the frequency in [Hz].

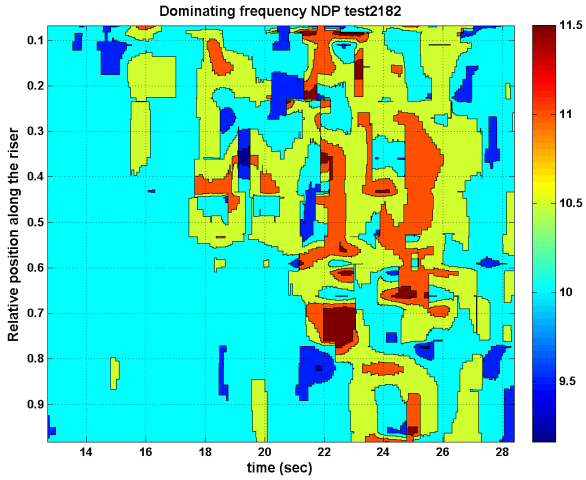

Figure A.8: Dominating frequencies for case 2182, velocity of current is 2.0m/s. Color scale on right hand side indicate the size of the frequency in [Hz]

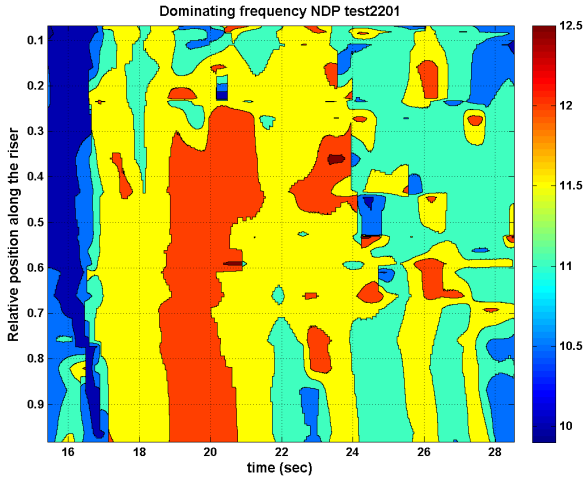

Figure A.9: Dominating frequencies for case 2201, velocity of current is 2.2m/s. Color scale on right hand side indicate the size of the frequency in [Hz]

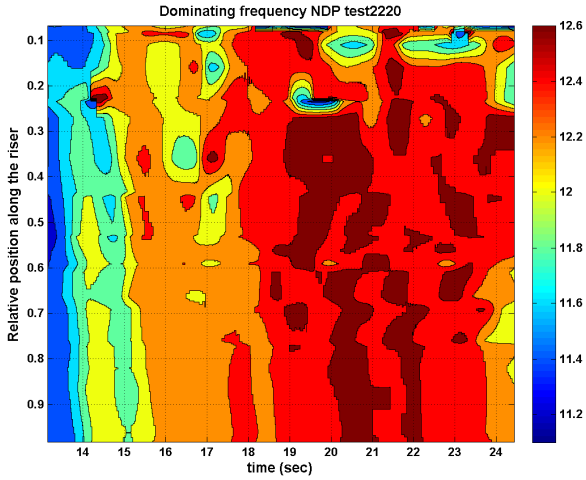

Figure A.10: Dominating frequencies for case 2220, velocity of current is 2.4m/s. Color scale on right hand side indicate the size of the frequency in [Hz]

A.2 Shear current

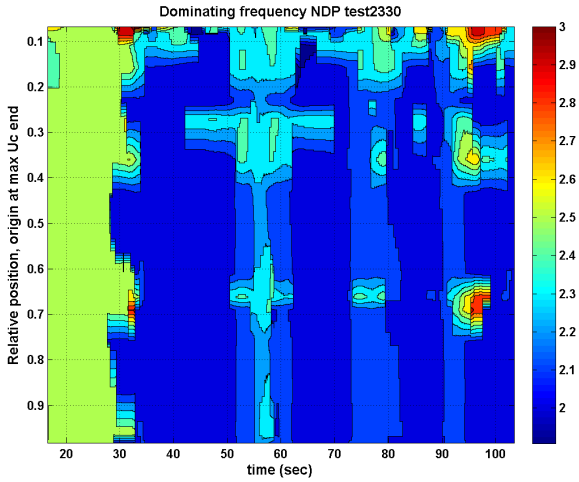

Figure A.11: Dominating frequencies for case 2330, max velocity of current is 0.5m/s. Color scale on right hand side indicate the size of the frequency in [Hz]

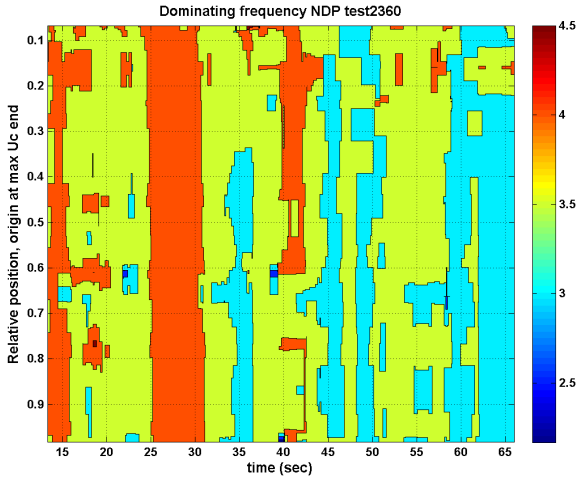

Figure A.12: Dominating frequencies for case 2360, max velocity of current is 0.8m/s. Color scale on right hand side indicate the size of the frequency in [Hz]

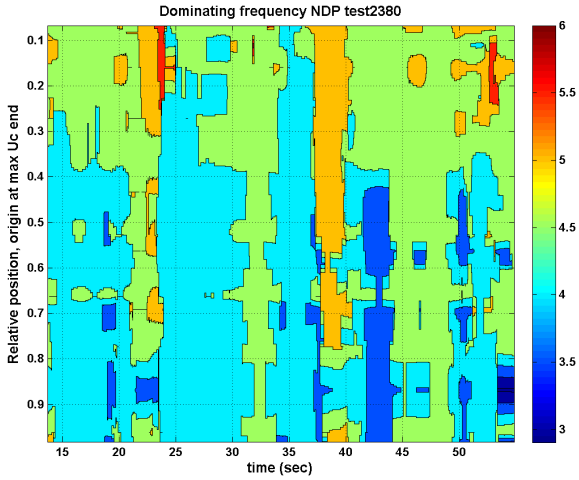

Figure A.13: Dominating frequencies for case 2380, max velocity of current is 1.0m/s. Color scale on right hand side indicate the size of the frequency in [Hz]

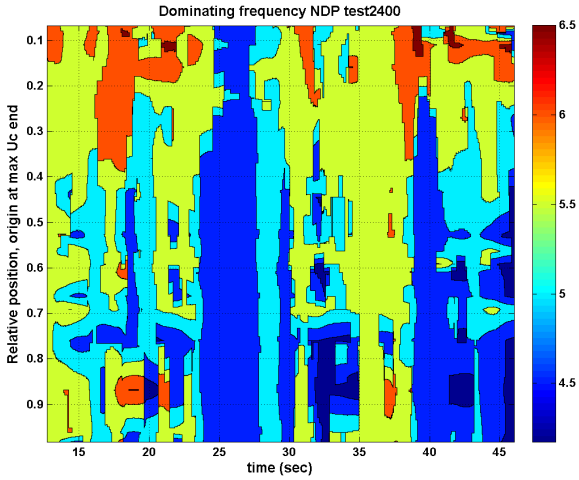

Figure A.14: Dominating frequencies for case 2400, max velocity of current is 1.2m/s. Color scale on right hand side indicate the size of the frequency in [Hz]

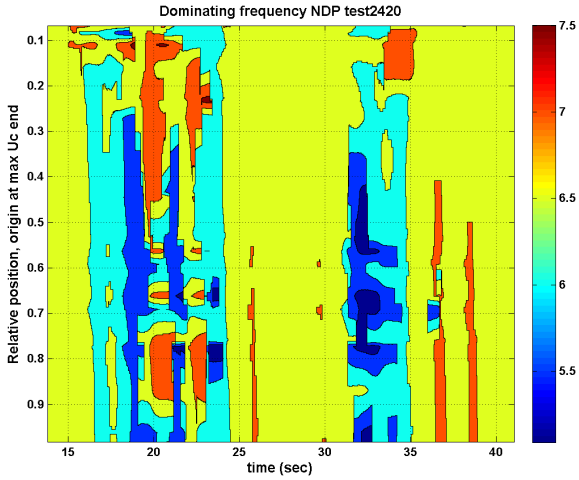

Figure A.15: Dominating frequencies for case 2420, max velocity of current is 1.4m/s. Color scale on right hand side indicate the size of the frequency in [Hz]

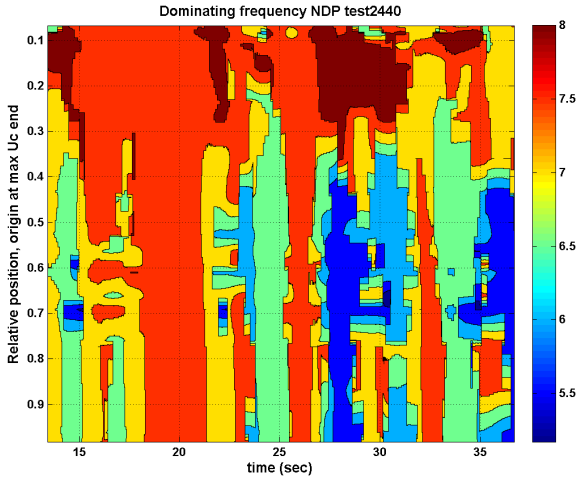

Figure A.16: Dominating frequencies for case 2440, max velocity of current is 1.6m/s. Color scale on right hand side indicate the size of the frequency in [Hz]

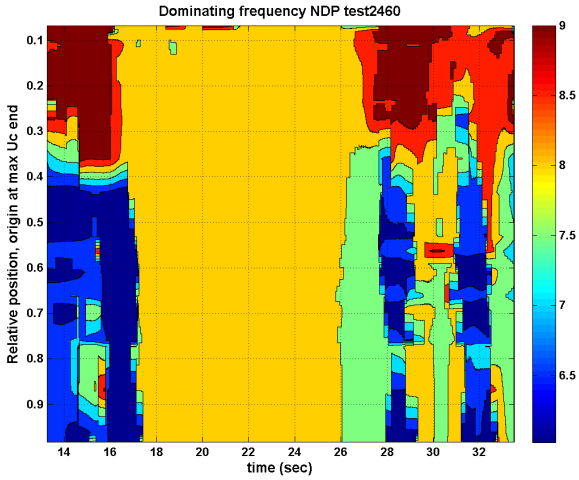

Figure A.17: Dominating frequencies for case 2460, max velocity of current is 1.8m/s. Color scale on right hand side indicate the size of the frequency in [Hz]

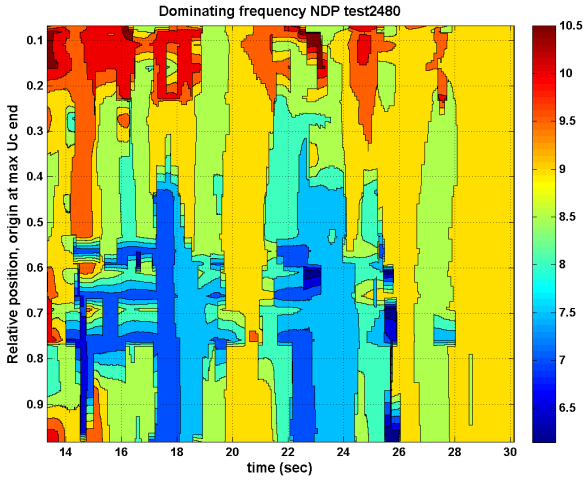

Figure A.18: Dominating frequencies for case 2480, max velocity of current is 2.0m/s. Color scale on right hand side indicate the size of the frequency in [Hz]

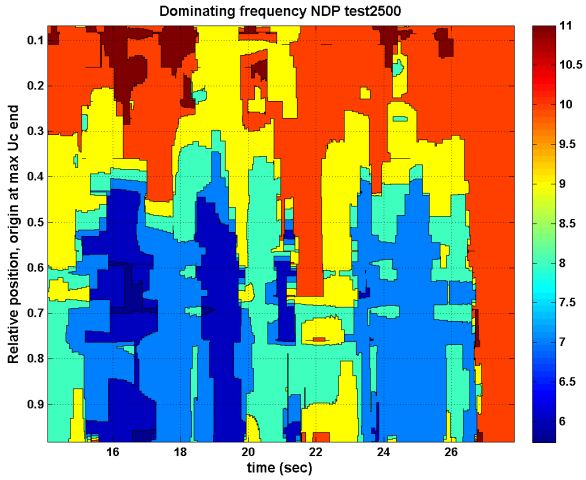

Figure A.19: Dominating frequencies for case 2500, max velocity of current is 2.2m/s. Color scale on right hand side indicate the size of the frequency in [Hz]

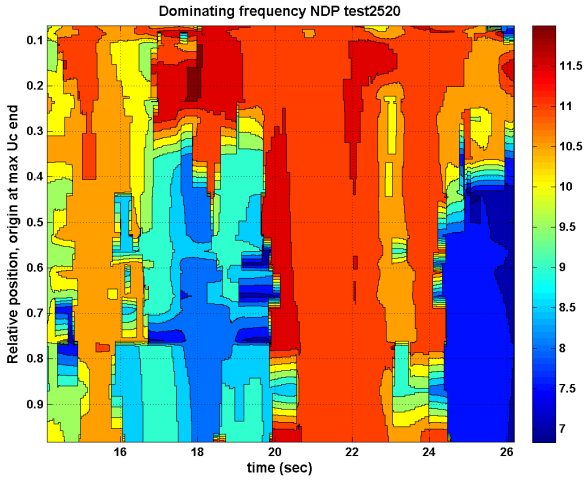

Figure A.20: Dominating frequencies for case 2520, max velocity of current is 2.4m/s. Color scale on right hand side indicate the size of the frequency in [Hz]

Appendix B

Amplitude plots

B.1 Uniform current

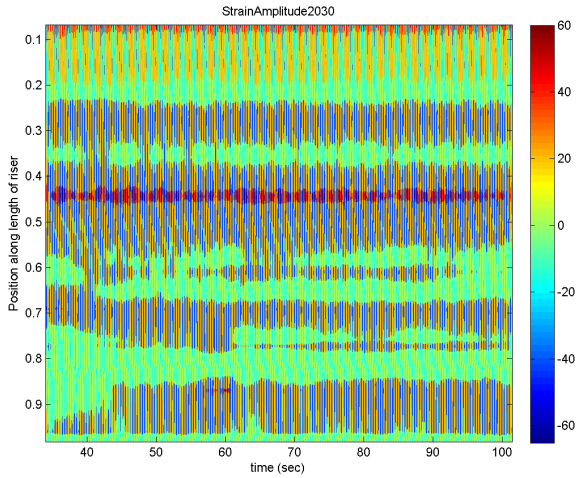

Figure B.1: Strain amplitudes for case 2030, velocity of current is 0.5m/s. Color scale on right hand side indicate the size of the strain-amplitude in [μm/m]

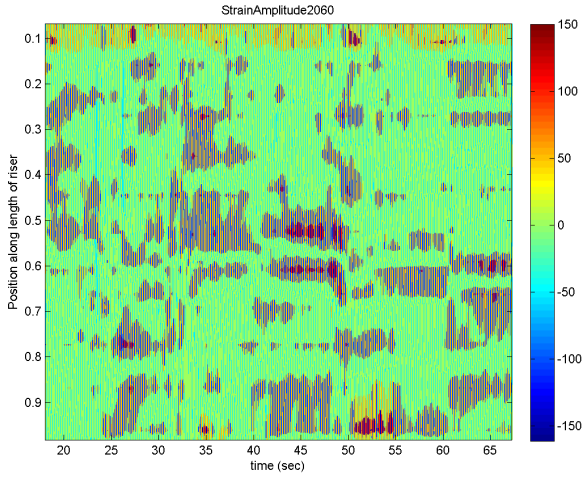

Figure B.2: Strain amplitudes for case 2060, velocity of current is 0.8m/s

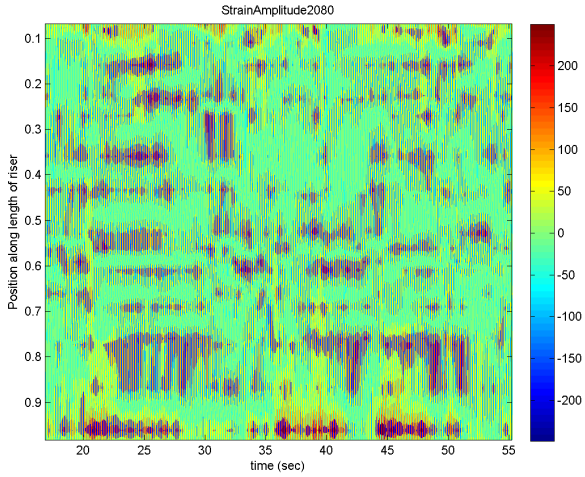

Figure B.3: Strain amplitudes for case 2080, velocity of current is 1.0m/s

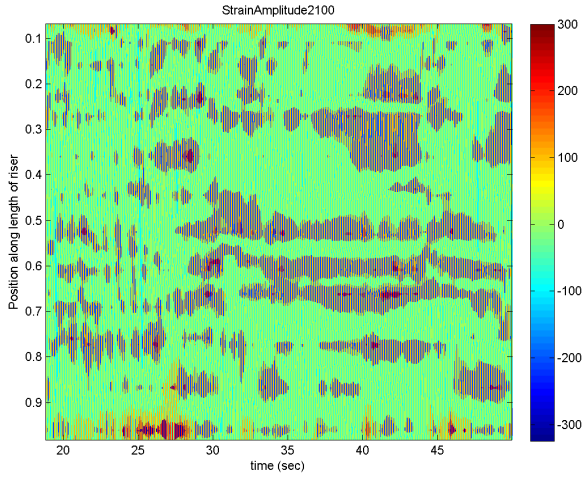

Figure B.4: Strain amplitudes for case 2100, velocity of current is 1.2m/s

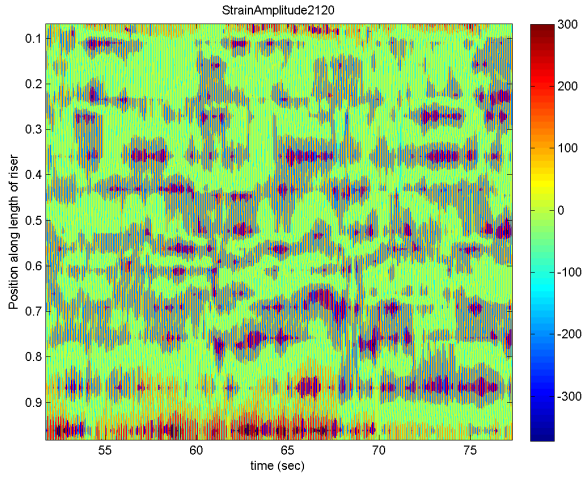

Figure B.5: Strain amplitudes for case 2120, velocity of current is 1.4m/s

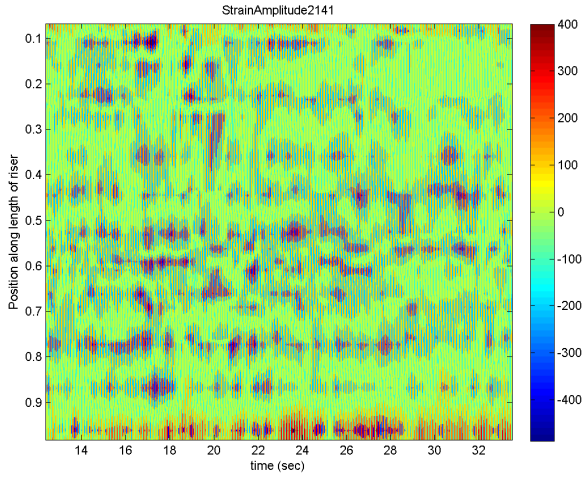

Figure B.6: Strain amplitudes for case 2141, velocity of current is 1.6m/s

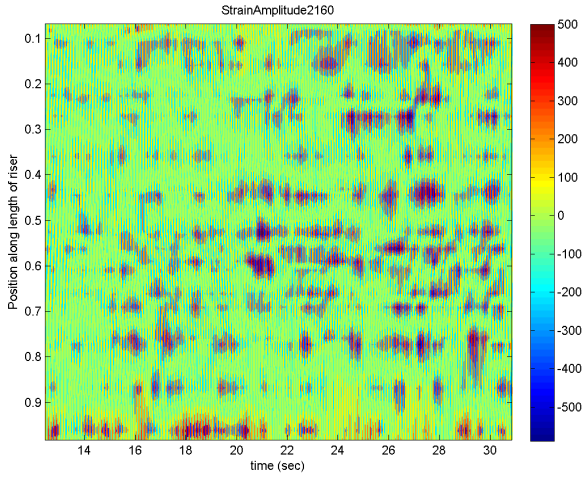

Figure B.7: Strain amplitudes for case 2160, velocity of current is 1.8m/s

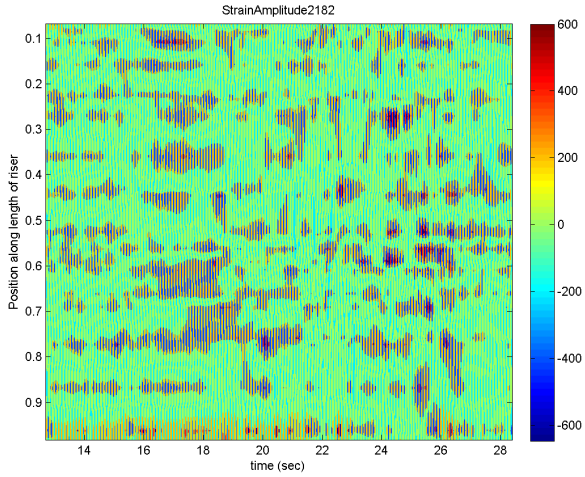

Figure B.8: Strain amplitudes for case 2182, velocity of current is 2.0m/s

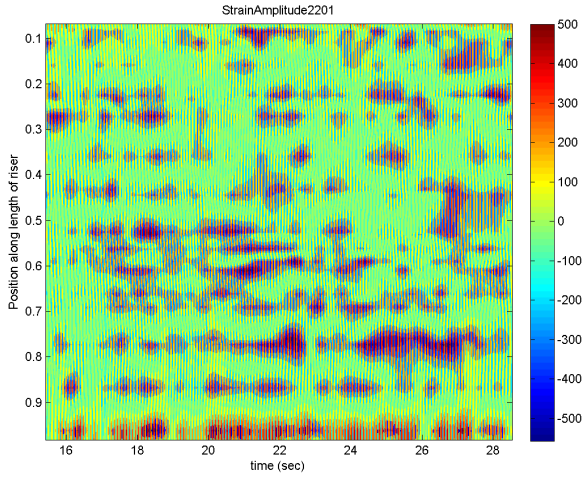

Figure B.9: Strain amplitudes for case 2201, velocity of current is 2.2m/s

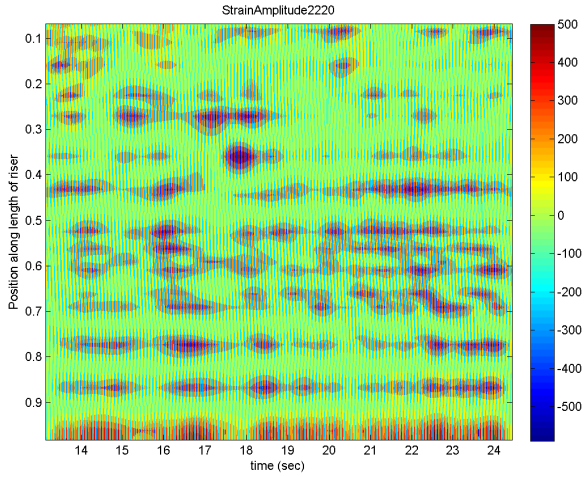

Figure B.10: Strain amplitudes for case 2220, velocity of current is 2.4m/s

B.2 Shear current

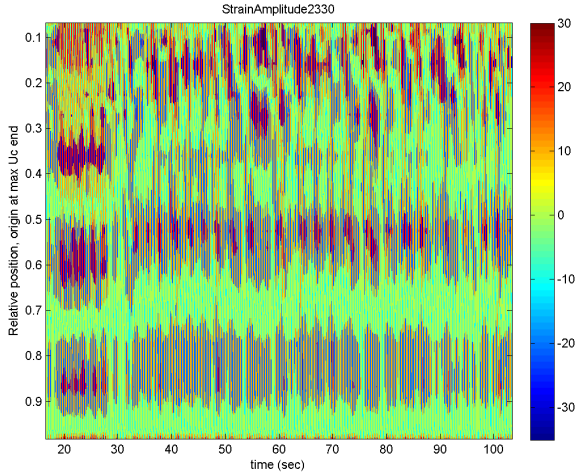

Figure B.11: Strain amplitudes for case 2330, max velocity of current is 0.5m/s

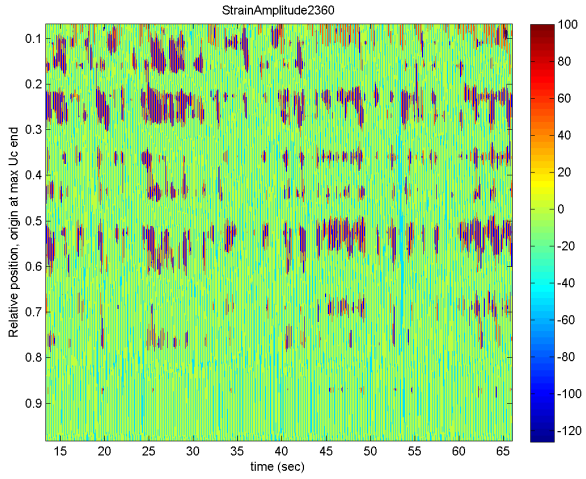

Figure B.12: Strain amplitudes for case 2360, max velocity of current is 0.8m/s

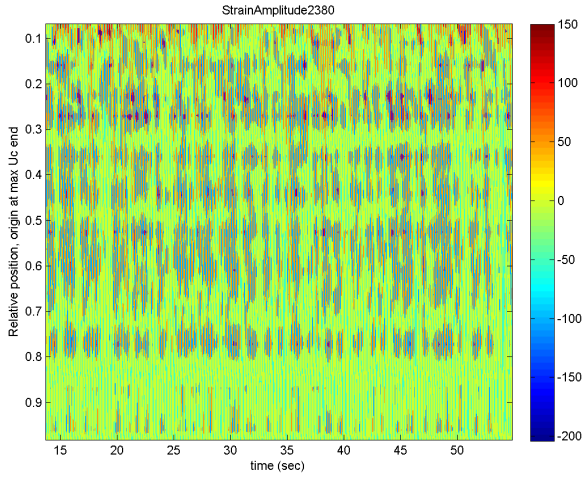

Figure B.13: Strain amplitudes for case 2380, max velocity of current is 1.0m/s

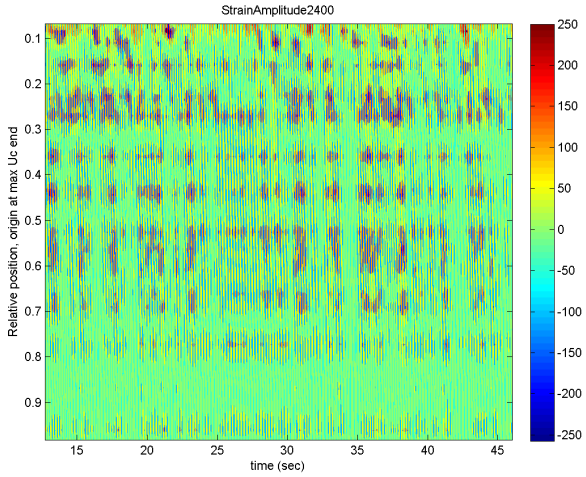

Figure B.14: Strain amplitudes for case 2400, max velocity of current is 1.2m/s

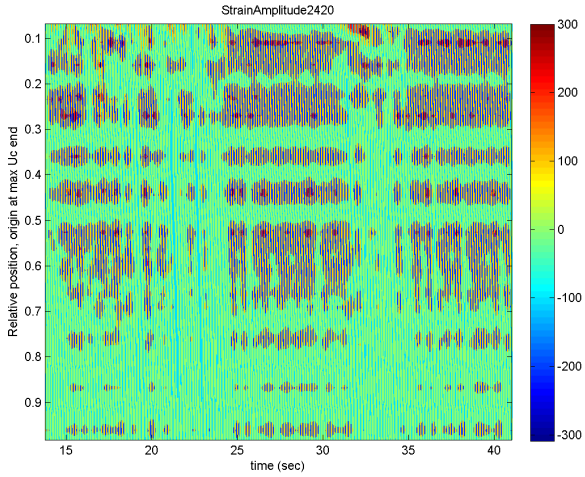

Figure B.15: Strain amplitudes for case 2420, max velocity of current is 1.4m/s

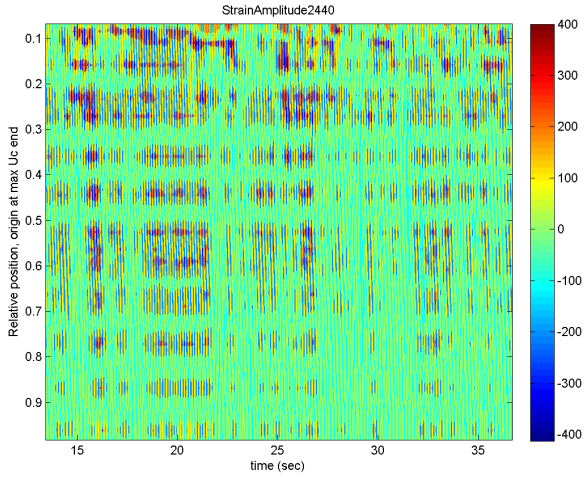

Figure B.16: Strain amplitudes for case 2440, max velocity of current is 1.6m/s

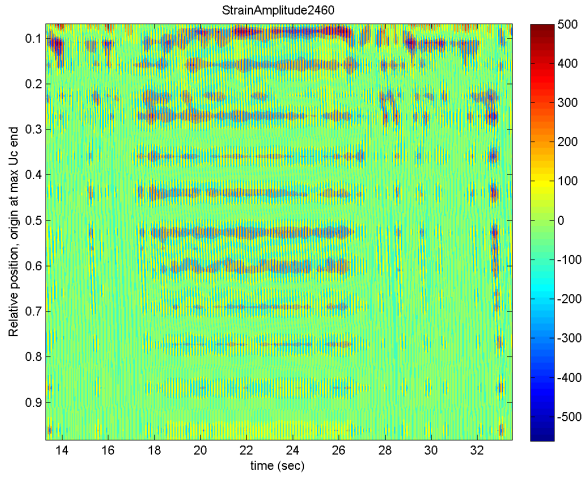

Figure B.17: Strain amplitudes for case 2460, max velocity of current is 1.8m/s

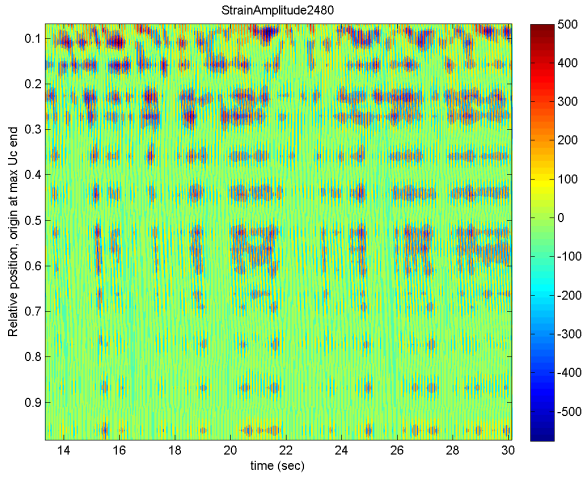

Figure B.18: Strain amplitudes for case 2480, max velocity of current is 2.0m/s

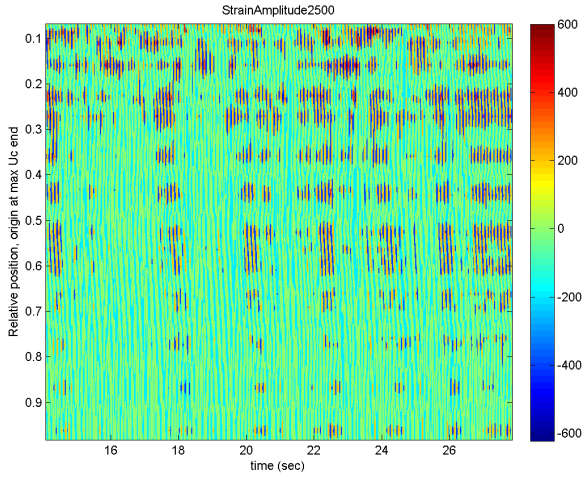

Figure B.19: Strain amplitudes for case 2500, max velocity of current is 2.2m/s

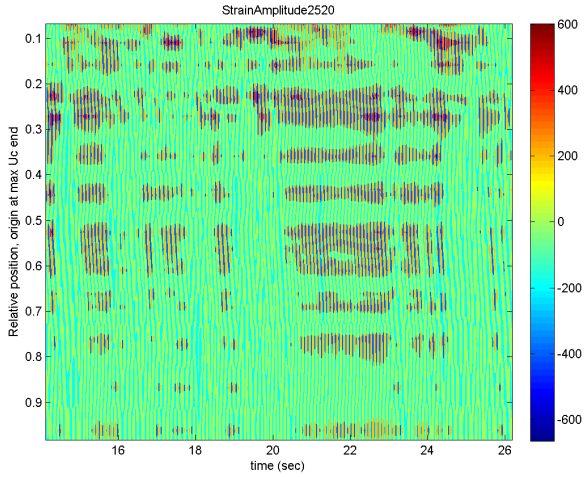

Figure B.20: Strain amplitudes for case 2520, max velocity of current is 2.4m/s

Appendix C

Tables

Added mass for the cases analysed									
Case #	Velocity, U [m/s] (shear: 2/3Umax)	mode no. (approx.)	Active freq. Min [1/s]	Active freq. Max [1/s]	Active freq. average,f [1/s]	Active freq. average, w [rad/s]	Tension [N]	Added mass [kg/m]	
2030	0.5	7	2.82	2.86	2.84	17.84424627	4067	3.358	
2060	0.8	8	4.2	4.75	4.475	28.11725425	4031	1.306	
2080	1	10	5.2	5.9	5.55	34.87167845	4044	1.354	U
2100	1.2	11	6	7.1	6.55	41.15486376	4125	1.096	N
2120	1.4	11	6.8	8	7.4	46.49557127	4291	0.720	I
2141	1.6	11	7.6	9	8.3	52.15043805	4584	0.470	F
2160	1.8	12	8.2	10	9.1	57.1769863	4688	0.489	O
2182	2	12	9.6	11.5	10.55	66.28760499	5095	0.216	R
2201	2.2	13	10.3	12	11.15	70.05751618	5602	0.396	M
2220	2.4	13	11.4	12.6	12	75.39822369	6285	0.353	
2330	0.33	4	2	2.5	2.25	14.13716694	4500	1.532	
2360	0.53	6	3	4	3.5	21.99114858	4500	1.361	
2380	0.67	8	3.5	5.4	4.45	27.96017462	4400	1.538	
2400	0.80	10	4.5	6	5.25	32.98672286	4350	1.815	S
2420	0.93	11	5.4	7	6.2	38.9557489	4300	1.427	H
2440	1.07	12	5.5	8	6.75	42.41150082	4300	1.440	E
2460	1.20	12	6.4	9	7.7	48.38052687	4325	0.901	A
2480	1.33	13	7	10	8.5	53.40707511	4375	0.856	R
2500	1.47	13	6.4	10.5	8.45	53.09291585	4425	0.898	
2520	1.60	13	7.5	11.5	9.5	59.69026042	4640	0.585	

Constant parameters		
pi	3.141592654	-
EI	37.22	Nm^2
L	38	m
mass, riser	0.933	kg/m

Table C.1: Overview of the calculations of added mass for all ten cases in uniform current and all ten cases in sheared current.

	Frequency [Hz]	Active period [s]	Relative period
case2330	2	19	0.23
	2.1	27.5	0.33
	2.3	14	0.17
	2.4	5	0.06
	2.5	18.3	0.22
		83.8	
case2360	3	10	0.19
	3.5	33.3	0.64
	4	9	0.17
		52.3	
case2380	4	8.4	0.20
	4.5	30.6	0.74
	5	2.2	0.05
		41.2	
case2400	4.5	5	0.15
	5	6.8	0.21
	5.5	18.6	0.56
	6	2.7	0.08
		33.1	
case2420	5.5	0.9	0.03
	6	6.5	0.24
	6.5	18.4	0.67
	7	1.5	0.05
		27.3	
case2440	6.5	3.8	0.16
	7	7.7	0.33
	7.5	11.1	0.47
	8	0.8	0.03
		23.4	
case2460	7.5	4.9	0.25
	8	11.1	0.56
	8.5	2.4	0.12
	9	1.5	0.08
		19.9	
case2480	7.5	0.2	0.01
	8	1.2	0.07
	8.5	5.3	0.33
	9	8.8	0.55
	9.5	0.6	0.04
		16.1	
case2500	8	0.1	0.01
	9	3.4	0.25
	10	9.4	0.69
	11	0.7	0.05
		13.6	
case2520	8.5	0.3	0.02
	9	0.3	0.02
	9.5	1.9	0.16
	10	0.9	0.07
	10.5	3.6	0.30
	11	4.6	0.38
	11.5	0.6	0.05
		12.2	

Table C.2: Data used for generating figure 5.5 in excel. Degree of time-participation of each active frequency is found from frequency-plots, at position corresponding to $2/3U_{max}$ for sheared current cases.

Uniform current		Sheared current	
Case no.	Towing velocity (current velocity) [m/s]	Case no.	Towing velocity (max current velocity) [m/s]
2030	0.5	2330	0.5
2060	0.8	2360	0.8
2080	1	2380	1
2100	1.2	2400	1.2
2120	1.4	2420	1.4
2141	1.6	2440	1.6
2160	1.8	2460	1.8
2182	2	2480	2
2201	2.2	2500	2.2
2220	2.4	2520	2.4

Table C.3: Overview of cases used in the analyses.